Modeling of two-phase flow in geophysics: compaction, differentiation, partial melting, and melt migration

Ondřej Šrámek
University of Maryland, Department of Geology

presented on Sep 18, 2012 at BIRS workshop
“Model reduction in continuum thermodynamics: Modeling, analysis and computation”
BIRS, Banff, Canada, Sep 16–21, 2012

Collaborators: David Bercovici, Stéphane Labrosse, Laura Milelli, Yanick Ricard

Geophysics, geodynamics

Earth & planets

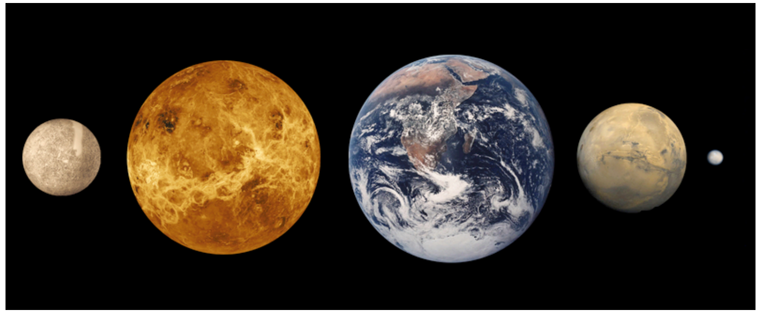

their evolution, formation, structure

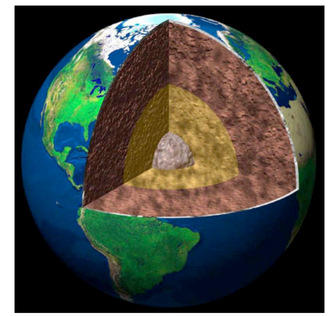

two-phase flow and deformation

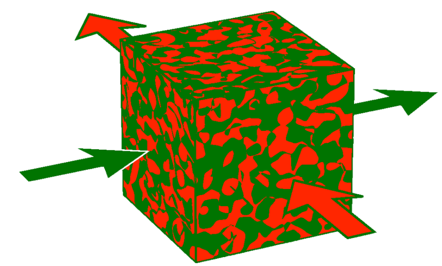

Outline

- geophysical motivation – multi-phase problems
- specific two-phase model
- applications
    - planetary core formation
    - coupling of deformation and melting

Earth structure

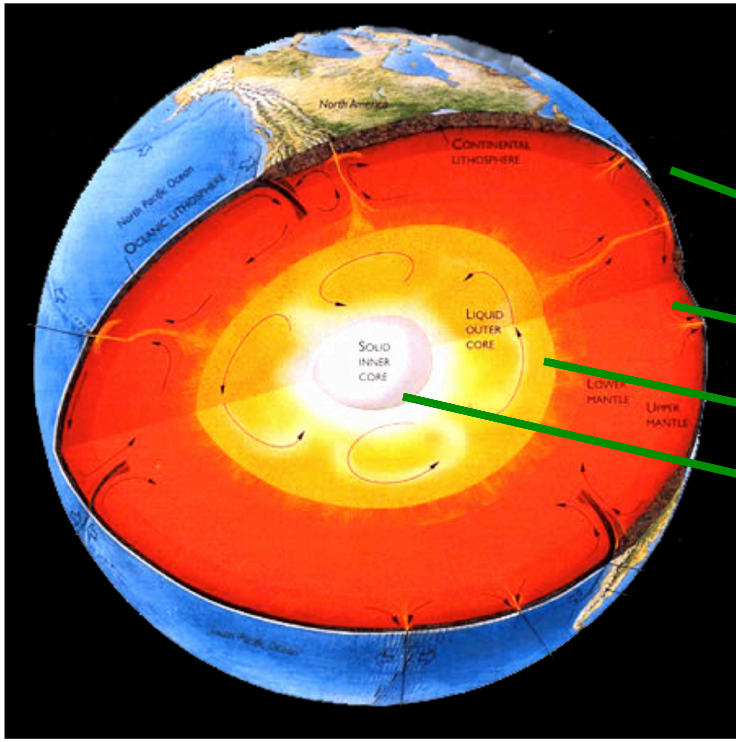

Differentiated (layered) structure

- crust ... light silicate rock
- mantle ... denser silicates
- outer core ... molten metal
- inner core ... solid iron

Dynamic interior – convection

- convection in molten outer core (geodynamo)
- convection in Earth mantle (plate tectonics at the surface)

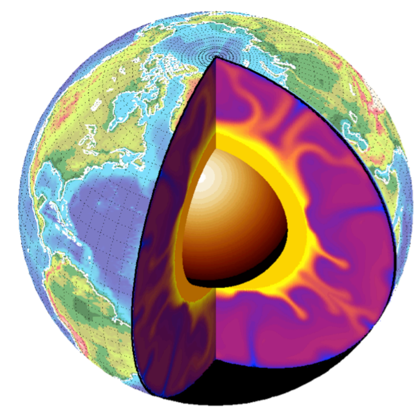

We have learned great deal using geodynamical modeling constrained by observations (seismology, gravity, geochemistry), realistic material parameters (high-pressure mineral physics). Single-/multi-phase models.

Shallow magmatism

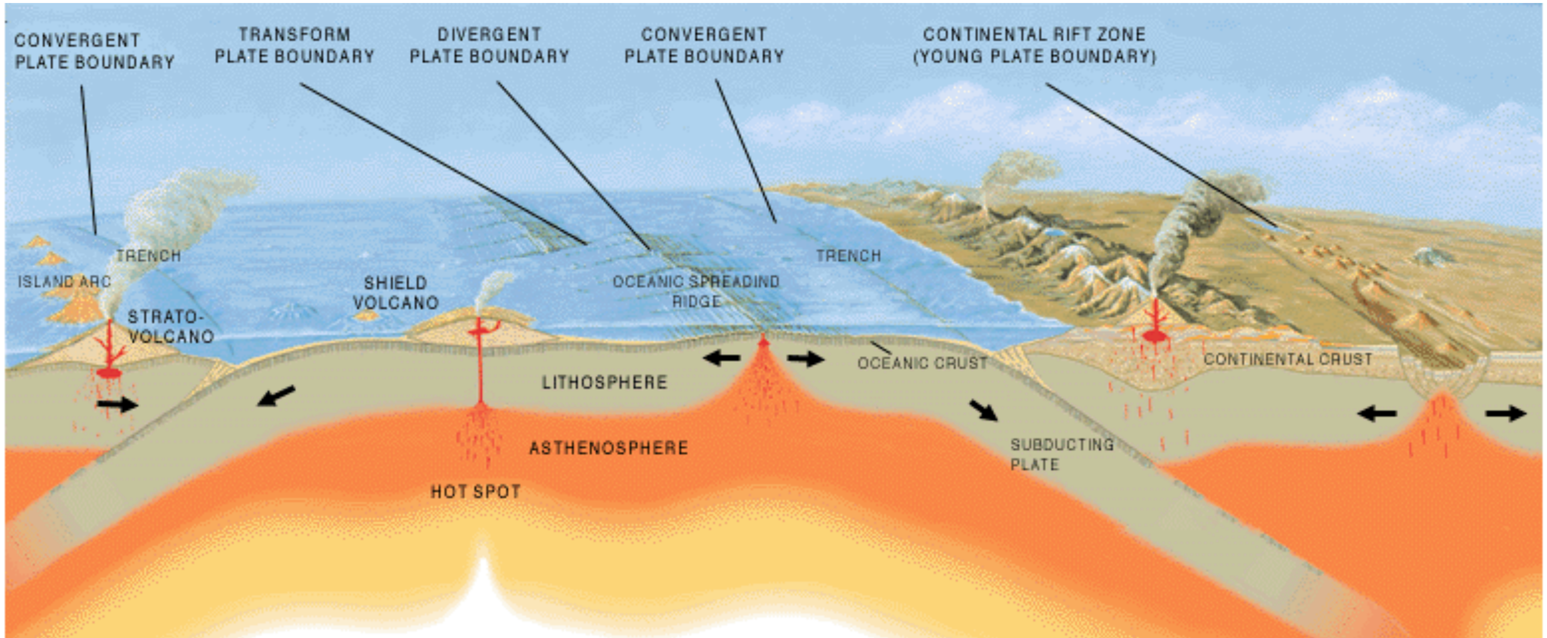

Figure modified after J. F.Vigil (USGS)

- mid-ocean ridges – pressure-release melting
- hot spots – melting due to high temperature
- arc volcanism – dehydration melting (composition)

Partially molten regions in deeper Earth (?)

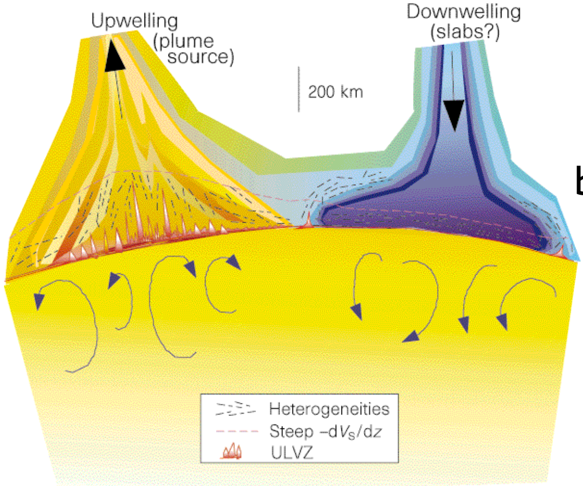

bottom of the mantle

~2900 km depth

top of the core

Lay et al. (1998)

bottom of Earth's mantle (~2800 km depth)

~400 km depth

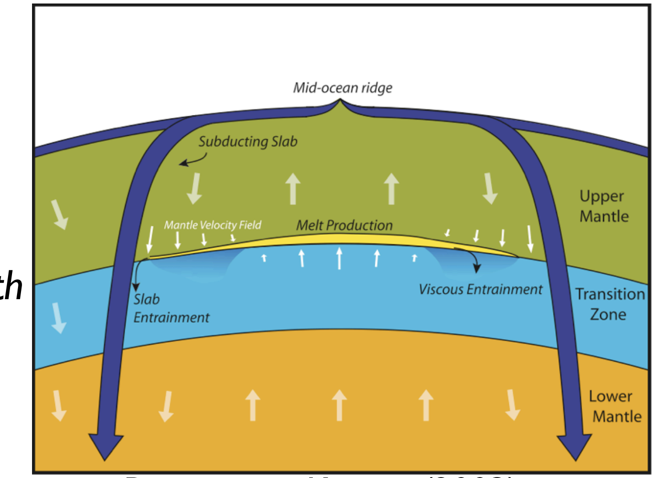

Bercovici & Karato (2003)

partial melt layer at ~400 km depth?

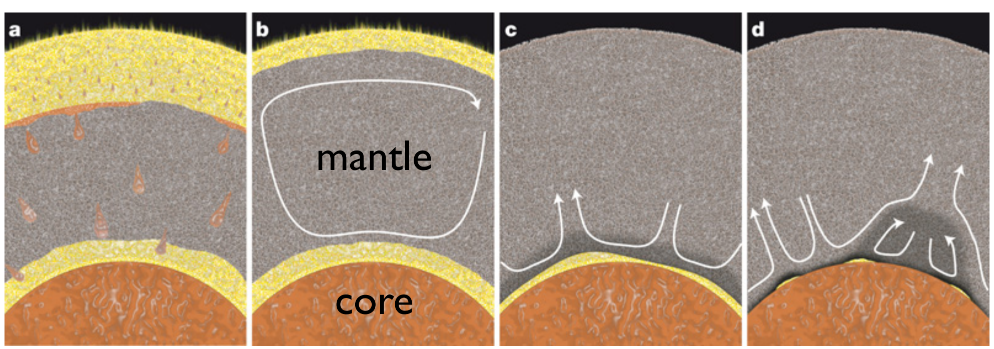

Labrosse et al. (2007)

basal magma ocean in the mantle

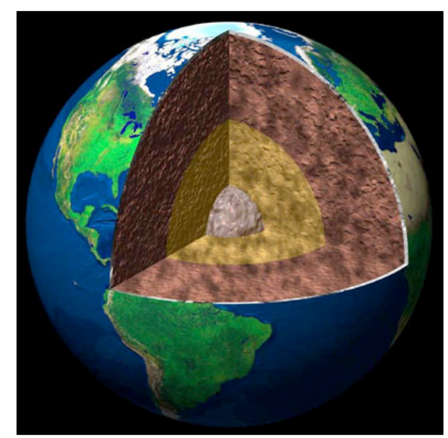

mushy layer at
inner core–outer core boundary

Planetary accretion and differentiation

- terrestrial planets: metallic core & silicate mantle
- the core–mantle differentiation during/after the late stage of planetary growth

building block
(chondtiric meteorite)

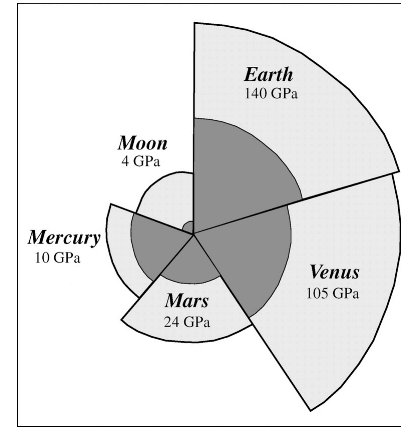

differentiated planets

nebula

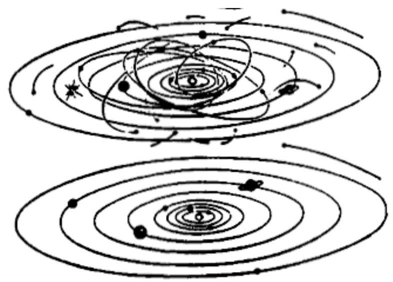

after Ahrens (1990)

High temperature conditions

Probably extensive melting

protoplanetary disk

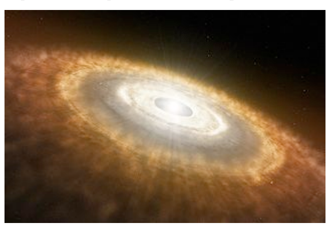

giant impacts

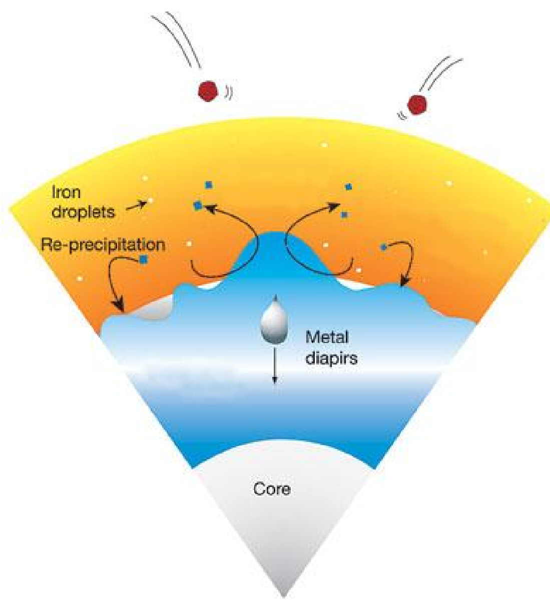

after Wood et al. (2007)

- accretion heat from impacts
- radiogenic heat from short-lived isotopes
- ΔT_{impact} may melt the metal, or even the silicates (magma ocean)
- easy differentiation if (partially) molten
- heating by differentiation
- further melting

Geophysical two-phase (multi-phase) problems

- partial melting: solid & melt (shallow & deep Earth)
  melt generation, migration, focussing, extraction
- planetary differentiation: silicate & metal
- other geoscience problems
  (e.g., icy satellites, glaciology, sediments and soils, fluid migration, hydrocarbon reservoirs and CO_2 sequestration, ...)
- phase vs. component ... grain/pore scale
- highly viscous flow ... acceleration, inertia neglected
  often a large difference in viscosities between phases

Two-phase models in geophysics

- effort to understand mid-ocean ridges
- early 70's (Sleep 1974, Turcotte & Ahern 1978, Ahern & Turcotte 1979)
- Mid 1980's:
- McKenzie (1984), Ribe (1985), Scott & Stevenson (1986)
  - general model of partially molten regions
  - porous flow of melt through viscous deformable matrix, or Darcy + deformation

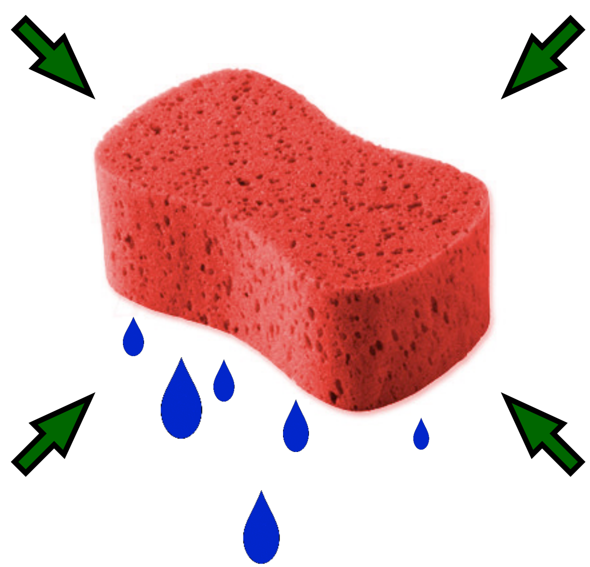

Recently developed two-phase model

- Bercovici, Ricard & Schubert (2001), Ricard & Bercovici (2003)
- accounts for the mechanical and thermodynamical effects of the interface (interfacial surface tension)
- requires a difference in pressures between the two phases
- phase change included (Šrámek et al. 2007)

Recently developed two-phase model

- Bercovici, Ricard & Schubert (2001), Ricard & Bercovici (2003)
- accounts for the mechanical and thermodynamical effects of the interface (interfacial surface tension)
- requires a difference in pressures between the two phases
- phase change included (Šrámek et al. 2007)

- Original motivation: non-equilibrium surface energy treatment
  → isotropic damage (void generation and growth)
  → description of weakening and shear localization
  → generation of plate tectonics
- I will not present the model in its most general form
- Will show a limited version – two-phase single-component model of compaction and phase change

Model assumptions

- each phase is an incompressible viscous fluid
- special case: very large viscosity ratio
- interaction: Darcy "fluid" flow through a deformable "matrix" ... interconnectivity

basaltic melt in olivine matrix

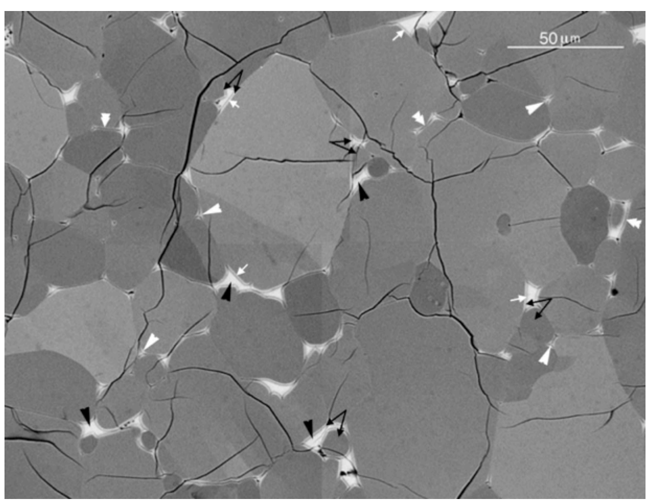

Cmíral et al. (1998)

FeS melt in solid metal

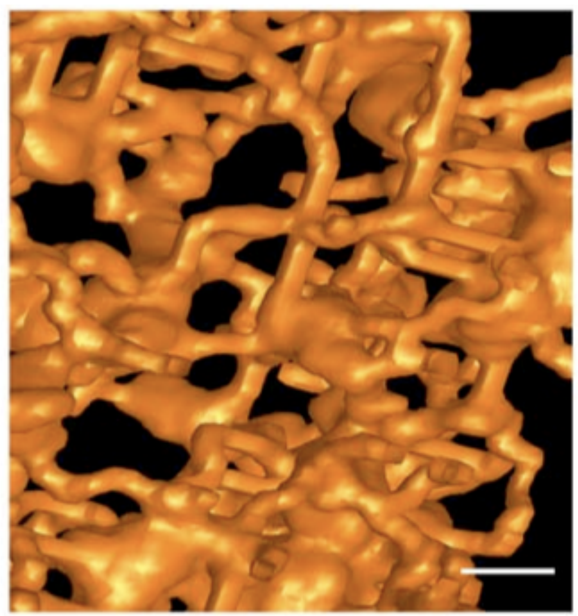

Roberts et al. (2007)

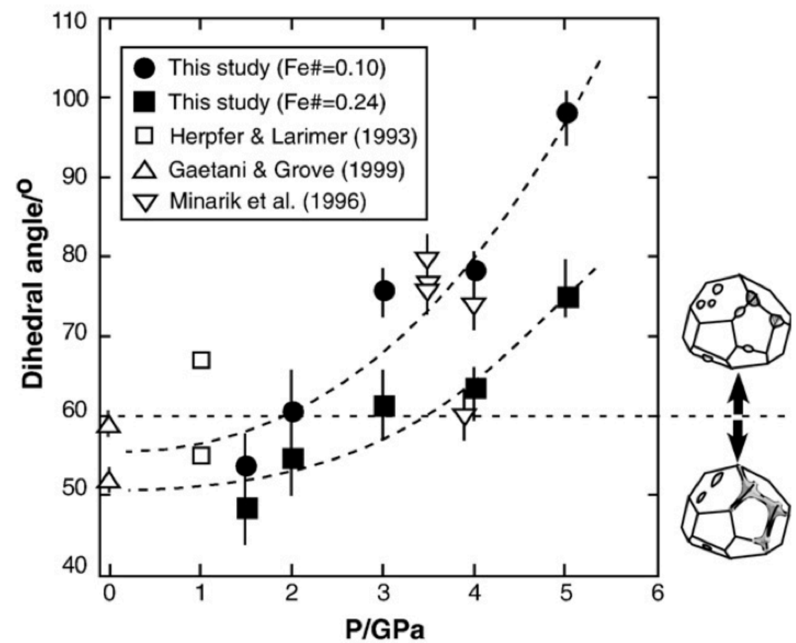

Terasaki et al. 2008

Two-phase continuum description

“fluid” phase ... index *f*

“matrix” phase ... index *m*

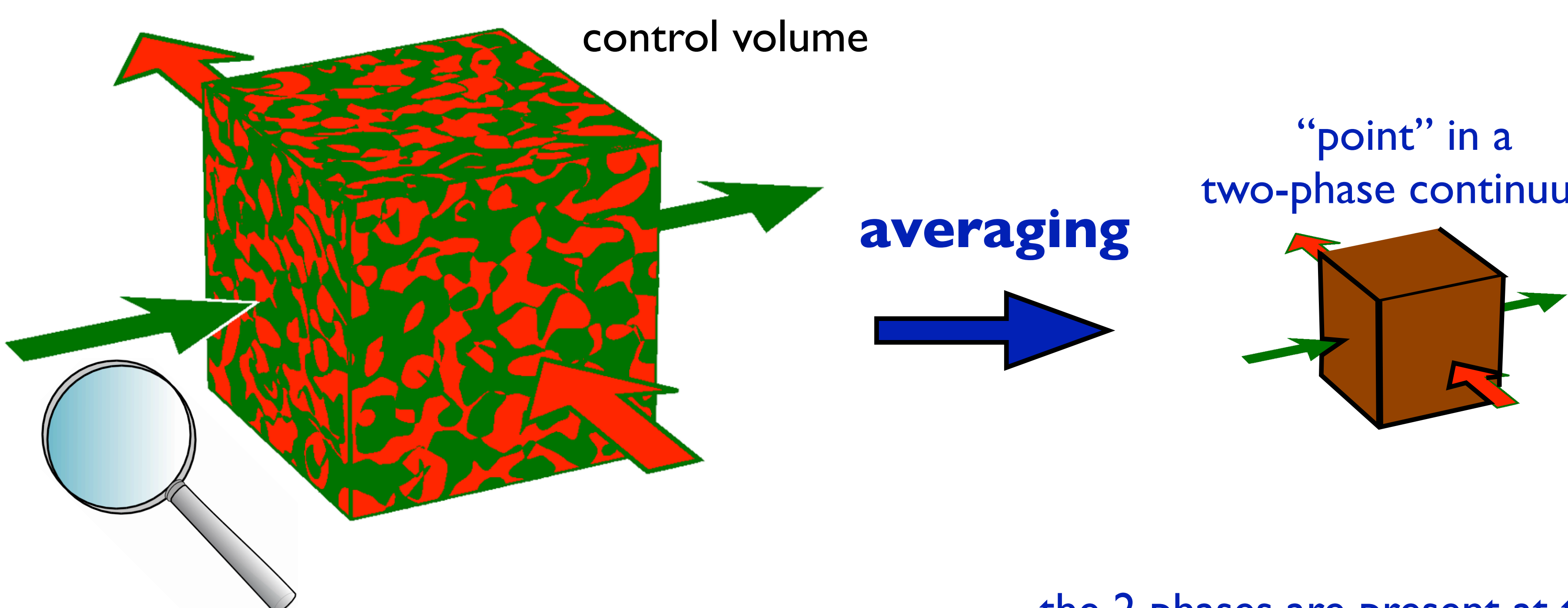

the 2 phases *f* and *m* occupy distinct regions at grain/pore scale

the 2 phases are present at the same “point” with volume fractions ϕ (porosity) and $1-\phi$

other quantities (e.g., velocities v_f, v_m) are also averaged and assumed continuous in space

Mass conservation

- incompressible viscous fluids
- matrix skeleton/fluid network "compressible"

$$\frac{\partial \phi}{\partial t} + \boldsymbol{\nabla} \cdot (\phi \mathbf{v}_f) = \frac{\Delta \Gamma}{\rho_f}$$

$$-\frac{\partial \phi}{\partial t} + \boldsymbol{\nabla} \cdot [(1-\phi)\mathbf{v}_m] = -\frac{\Delta \Gamma}{\rho_m}$$

- porosity Φ
- averaged velocities v_m, v_f
- melting rate $\Delta\Gamma$
- densities ρ_m, ρ_f

Momentum equations

force balance for the individual phases in the limit $\mu_f << \mu_m$
inertial terms neglected

generalized Darcy's law

$$-\phi\underline{[\nabla P_f - \rho_f \mathbf{g}]} + c\boldsymbol{\Delta}\mathbf{v} = 0$$

↑ non-hydrostatic pressure gradient

interaction coefficient (cf. Darcy's law)

$$c = \frac{\mu_f \phi^2}{k(\phi)} = \frac{\mu_f}{k_0}$$

permeability exponent = 2

matrix momentum equation

$$-(1-\phi)[\nabla P_m - \rho_m \mathbf{g}] + \nabla \cdot [(1-\phi)\underline{\boldsymbol{\tau}}_m] - c\boldsymbol{\Delta}\mathbf{v} + \Delta P \nabla\phi + \nabla(\sigma\alpha) = 0$$

interfacial surface tension: $\nabla(\sigma\alpha)$

coefficient of surface tension: σ

interfacial area density: α

deviatoric viscous stress in the matrix

$$\boldsymbol{\tau}_m = \mu_m \left(\nabla \mathbf{v}_m + [\nabla \mathbf{v}_m]^T - \frac{2}{3}\nabla \cdot \mathbf{v}_m \mathbf{I} \right)$$

Energy balance for the two-phase mixture

thermal equilibrium between the phases

phase *f* — phase *m* — interfacial terms

$$\phi\rho_f C_f \frac{\mathrm{D}_f T}{\mathrm{D}t} + (1-\phi)\rho_m C_m \frac{\mathrm{D}_m T}{\mathrm{D}t} - T\frac{\mathrm{D}_m}{\mathrm{D}t}\left(\alpha\frac{\mathrm{d}\sigma}{\mathrm{d}T}\right) - T\alpha\frac{\mathrm{d}\sigma}{\mathrm{d}T}\boldsymbol{\nabla}\cdot\mathbf{v}_m$$

$$= -T\Delta s\Delta\Gamma + Q - \boldsymbol{\nabla}\cdot\mathbf{q} + \Psi - \left(\Delta P + \sigma\frac{\mathrm{d}\alpha}{\mathrm{d}\phi}\right)\frac{\mathrm{D}_m\phi}{\mathrm{D}t} + \left(\Delta\varepsilon - T\Delta s + \frac{P_m}{\rho_m} - \frac{P_f}{\rho_f}\right)\Delta\Gamma$$

- $-T\Delta s\Delta\Gamma$: latent heat
- Q: radiogenic heat
- $-\boldsymbol{\nabla}\cdot\mathbf{q}$: heat diffusion
- $\left(\Delta P + \sigma\frac{\mathrm{d}\alpha}{\mathrm{d}\phi}\right)\frac{\mathrm{D}_m\phi}{\mathrm{D}t}$: heat source related to change in porosity
- $\left(\Delta\varepsilon - T\Delta s + \frac{P_m}{\rho_m} - \frac{P_f}{\rho_f}\right)\Delta\Gamma$: heat source related to phase change

$$\Psi = c\Delta v^2 + (1-\phi)\boldsymbol{\nabla}\mathbf{v}_m : \underline{\boldsymbol{\tau}}_m$$ dissipative heating

Energy balance for the two-phase mixture

thermal equilibrium between the phases

phase *f* — phase *m* — interfacial terms

$$\phi\rho_f C_f \frac{\mathrm{D}_f T}{\mathrm{D}t} + (1-\phi)\rho_m C_m \frac{\mathrm{D}_m T}{\mathrm{D}t} - T\frac{\mathrm{D}_m}{\mathrm{D}t}\left(\alpha\frac{\mathrm{d}\sigma}{\mathrm{d}T}\right) - T\alpha\frac{\mathrm{d}\sigma}{\mathrm{d}T}\boldsymbol{\nabla}\cdot\mathbf{v}_m$$

$$= -T\Delta s\Delta\Gamma + Q - \boldsymbol{\nabla}\cdot\mathbf{q} + \Psi - \left(\Delta P + \sigma\frac{\mathrm{d}\alpha}{\mathrm{d}\phi}\right)\frac{\mathrm{D}_m\phi}{\mathrm{D}t} + \left(\Delta\varepsilon - T\Delta s + \frac{P_m}{\rho_m} - \frac{P_f}{\rho_f}\right)\Delta\Gamma$$

- latent heat
- radiogenic heat
- heat diffusion
- heat source related to change in porosity
- heat source related to phase change

$$\Psi = c\Delta v^2 + (1-\phi)\boldsymbol{\nabla}\mathbf{v}_m : \underline{\boldsymbol{\tau}}_m$$ dissipative heating

9 equations written

mass, momentum, energy

but 11 unknowns

2 velocities, 2 pressures, temperature, porosity, melting rate

non-equilibrium thermodynamics provides 2 additional relations

Non-equilibrium thermodynamics

flux | force

$$\begin{pmatrix} \frac{\mathrm{D}_m \phi}{\mathrm{D}t} \\ \Delta\Gamma \end{pmatrix} = \begin{pmatrix} \cdot & \cdot \\ \cdot & \cdot \end{pmatrix} \begin{pmatrix} -\Delta P - \sigma \frac{\mathrm{d}\alpha}{\mathrm{d}\phi} \\ \Delta\varepsilon - T\Delta s + \frac{P_m}{\rho_m} - \frac{P_f}{\rho_f} \end{pmatrix}$$

2nd law of thermodynamics
Onsager's relations
micromechanical model
limiting cases

relation for pressure difference

$\frac{\mathrm{d}\alpha}{\mathrm{d}\phi}$ sum of principal interface curvatures

$$\Delta P + \sigma \frac{\mathrm{d}\alpha}{\mathrm{d}\phi} = -\frac{4}{3}\frac{\mu_m}{\phi} \boldsymbol{\nabla} \cdot \mathbf{v}_m$$

deviation of pressure difference from the static Laplace's condition $\propto$ compaction/dilation of the matrix

kinetic relation for melting rate

$$\Delta\Gamma = \chi \left(\Delta\varepsilon - T\Delta s - P_f \frac{\Delta\rho}{\rho_f \rho_m} - \frac{\sigma}{\rho_m}\frac{\mathrm{d}\alpha}{\mathrm{d}\phi} \right)$$

melting rate $\propto$ departure from equilibrium

Šrámek et al. (2007)

Overview of the model

$$\frac{\partial \phi}{\partial t} + \boldsymbol{\nabla} \cdot [\phi \mathbf{v}_f] = \frac{\Delta\Gamma}{\rho_f}$$

$$-\frac{\partial \phi}{\partial t} + \boldsymbol{\nabla} \cdot [(1-\phi)\mathbf{v}_m] = -\frac{\Delta\Gamma}{\rho_m}$$

mass (2x)

$$-\phi[\boldsymbol{\nabla} P_f - \rho_f \mathbf{g}] + c\boldsymbol{\Delta}\mathbf{v} = 0$$

$$-(1-\phi)[\boldsymbol{\nabla} P_m - \rho_m \mathbf{g}] + \boldsymbol{\nabla} \cdot [(1-\phi)\underline{\boldsymbol{\tau}}_m] - c\boldsymbol{\Delta}\mathbf{v} + \Delta P \boldsymbol{\nabla}\phi = 0$$

momentum (2x)

$$\phi\rho_f C_f \frac{\mathrm{D}_f T}{\mathrm{D}t} + (1-\phi)\rho_m C_m \frac{\mathrm{D}_m T}{\mathrm{D}t} = -T\Delta s \Delta\Gamma + Q - \boldsymbol{\nabla}\cdot\mathbf{q} + \Psi + \frac{4}{3}\mu_m \frac{1-\phi}{\phi}(\boldsymbol{\nabla}\cdot\mathbf{v}_m)^2 + \frac{\Delta\Gamma^2}{\chi}$$

energy

$$\Delta P = -\frac{4}{3}\frac{\mu_m}{\phi}\boldsymbol{\nabla}\cdot\mathbf{v}_m$$

pressure difference

$$\Delta\Gamma = \chi\left(\Delta\varepsilon - T\Delta s - P_f \frac{\Delta\rho}{\rho_f \rho_m}\right)$$

melting rate

$$\boldsymbol{\tau}_m = \mu_m\left(\boldsymbol{\nabla}\mathbf{v}_m + [\boldsymbol{\nabla}\mathbf{v}_m]^T - \frac{2}{3}\boldsymbol{\nabla}\cdot\mathbf{v}_m \mathbf{I}\right)$$

rheology

Šrámek et al. (2007)

Two-phase model for geophysical flows

- consistent description of mechanics and thermodynamics of a deforming two-phase medium
- includes phase change (melting/freezing)
- accounts for coupling between phase change, interfacial effects and viscous deformation
- set of continuum mechanics PDEs
- generalization: multi-component (Rudge et al. 2011)

Application 1: metal–silicate segregation and core formation

Accreting planetesimal

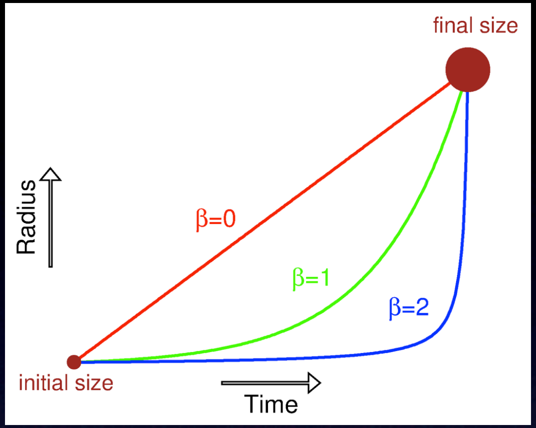

Examples of thermal structure (no differentiation)

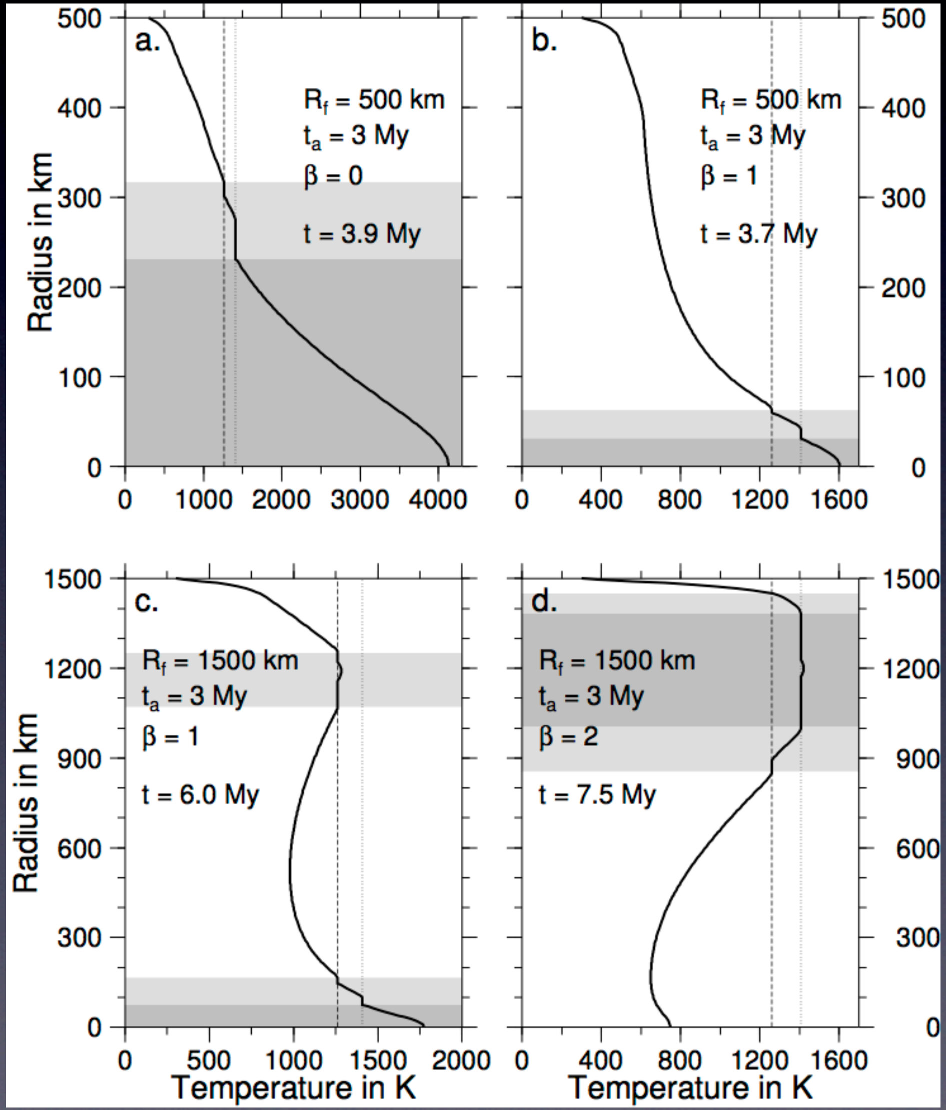

- radiogenic heating – ^{26}Al, 0.74 My half-life, volumetric
- impactor heating (gravitational) – near-surface

smaller final size,
melting from the center outward

larger final size,
strong near-surface heating

melting => differentiation

Šrámek et al. (2012)

Thermal evolution with differentiation

- spherically symmetric case
- initial state: cold (all solid), 20% metal & 80% silicate
- porous flow and deformation if partially molten
  or ~instantaneous separation when fully molten

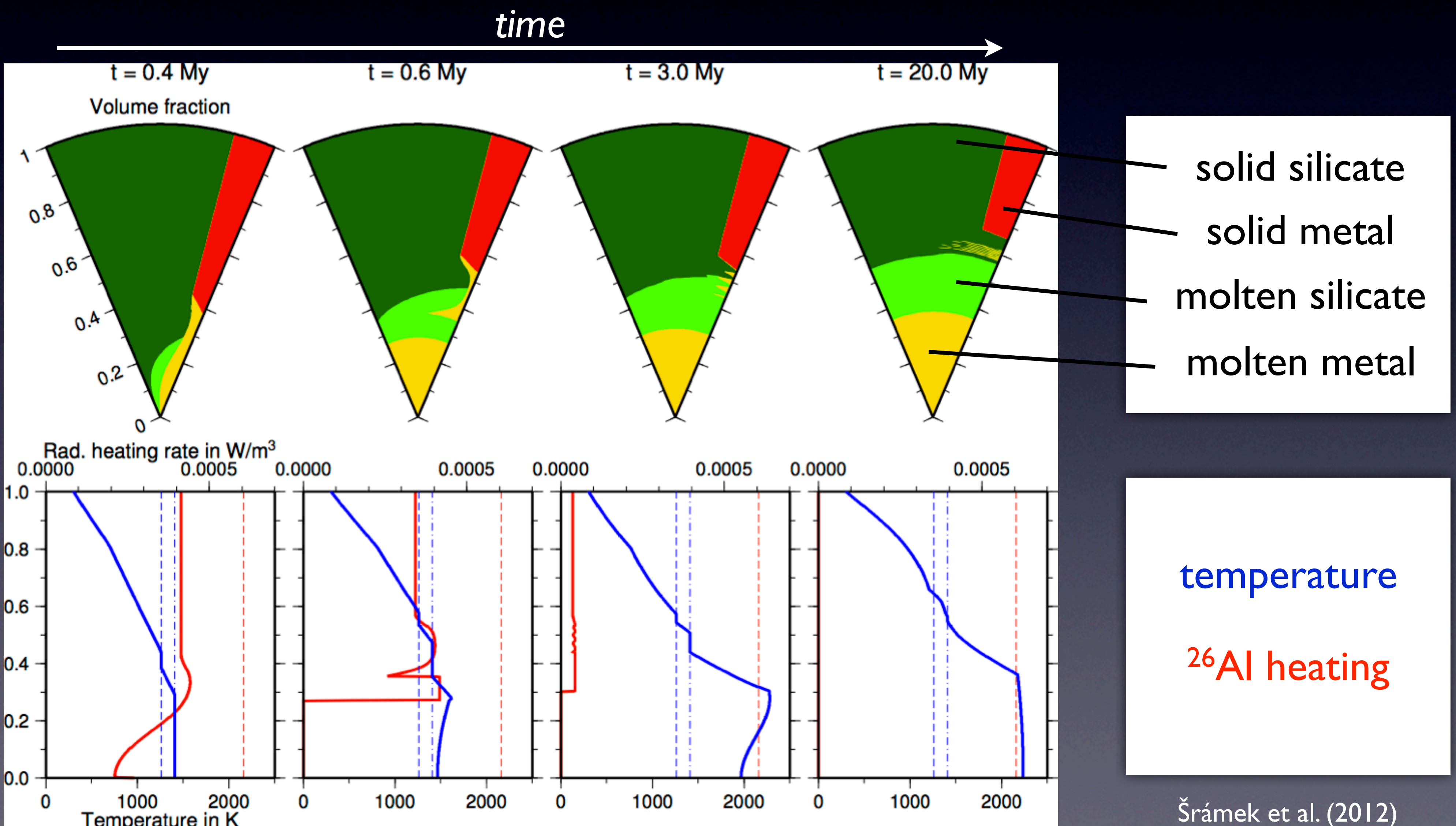

Šrámek et al. (2012)

2-D Cartesian model of core formation

- solved using finite differences on a staggered grid

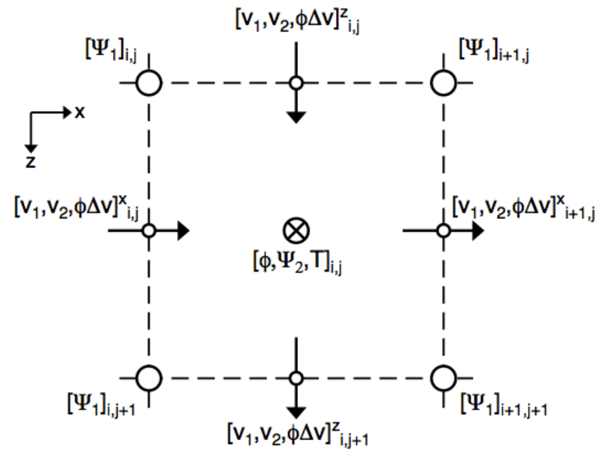

$$\phi(\mathbf{v}_f - \mathbf{v}_m)$$

- =0 if metal solid ... single phase
- ≠0 if metal molten ... phases separate

Simplifications

- silicates never melt
- viscosities of the silicates and solid metal are equal

Ricard et al. (2009), Šrámek et al. (2010)

2-D Cartesian model – numerical method

average momentum equation:
direct solver (F. Dubuffet)

Darcy separation and compaction:
ADI iterative

porosity advection:
TVD flux limiter scheme

initial porosity | 2π-rotation: upwind | 2π-rotation: our method

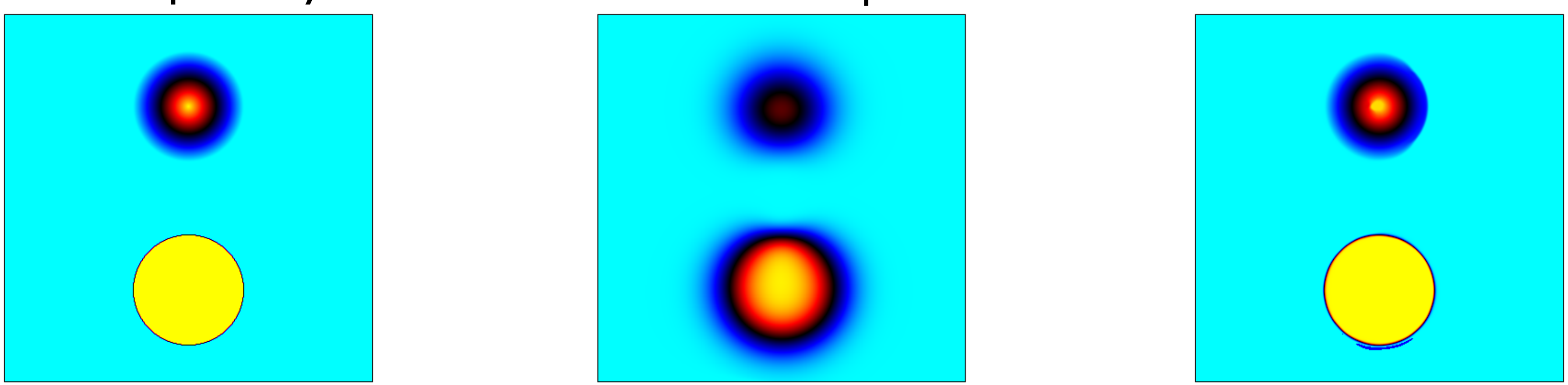

Ricard et al. (2009), Šrámek et al. (2010)

Simulation of an impact-induced differentiation

fraction of metal ϕ | temperature T

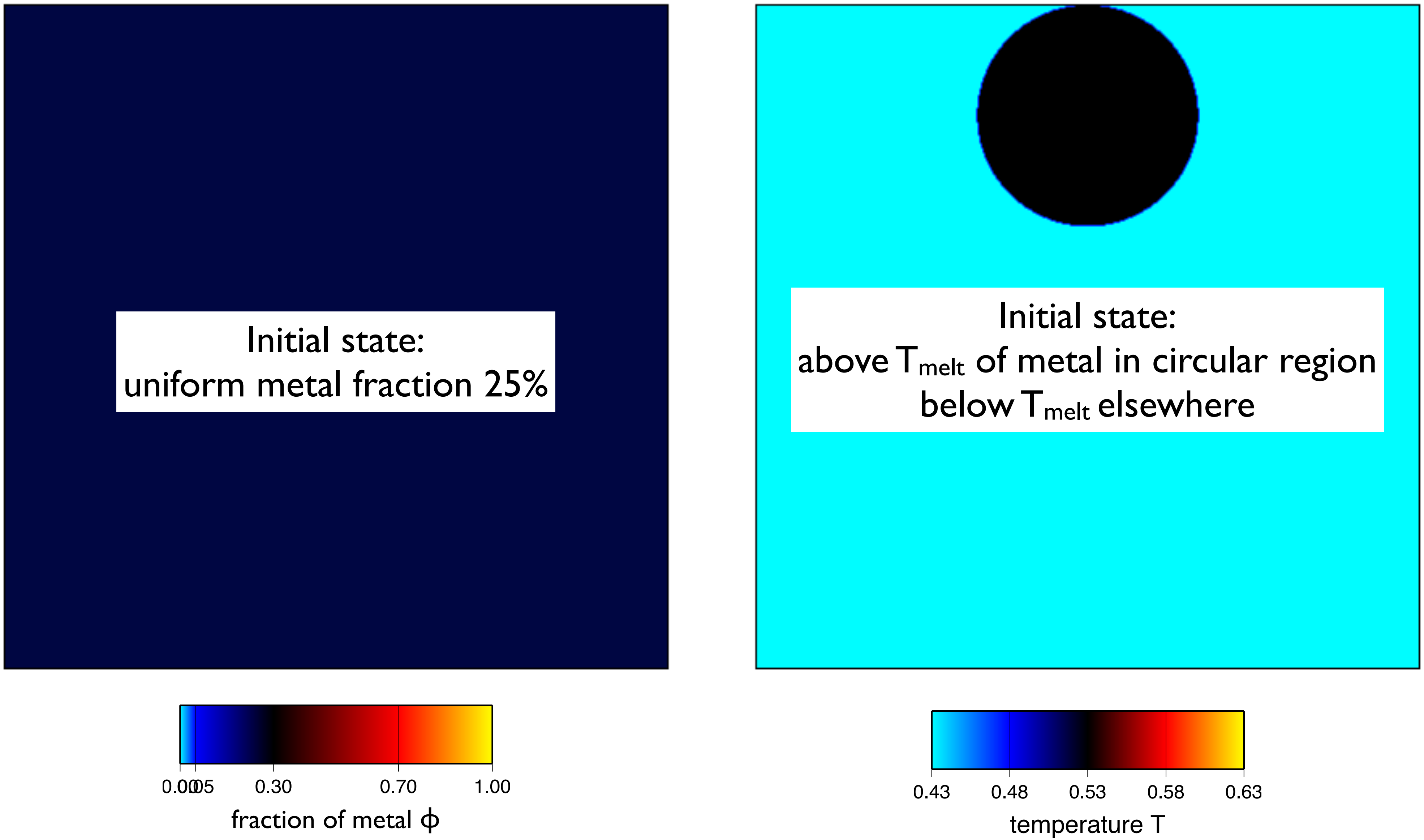

Ricard et al. (2009), Šrámek et al. (2010)

Simulation of an impact-induced differentiation

fraction of metal ϕ

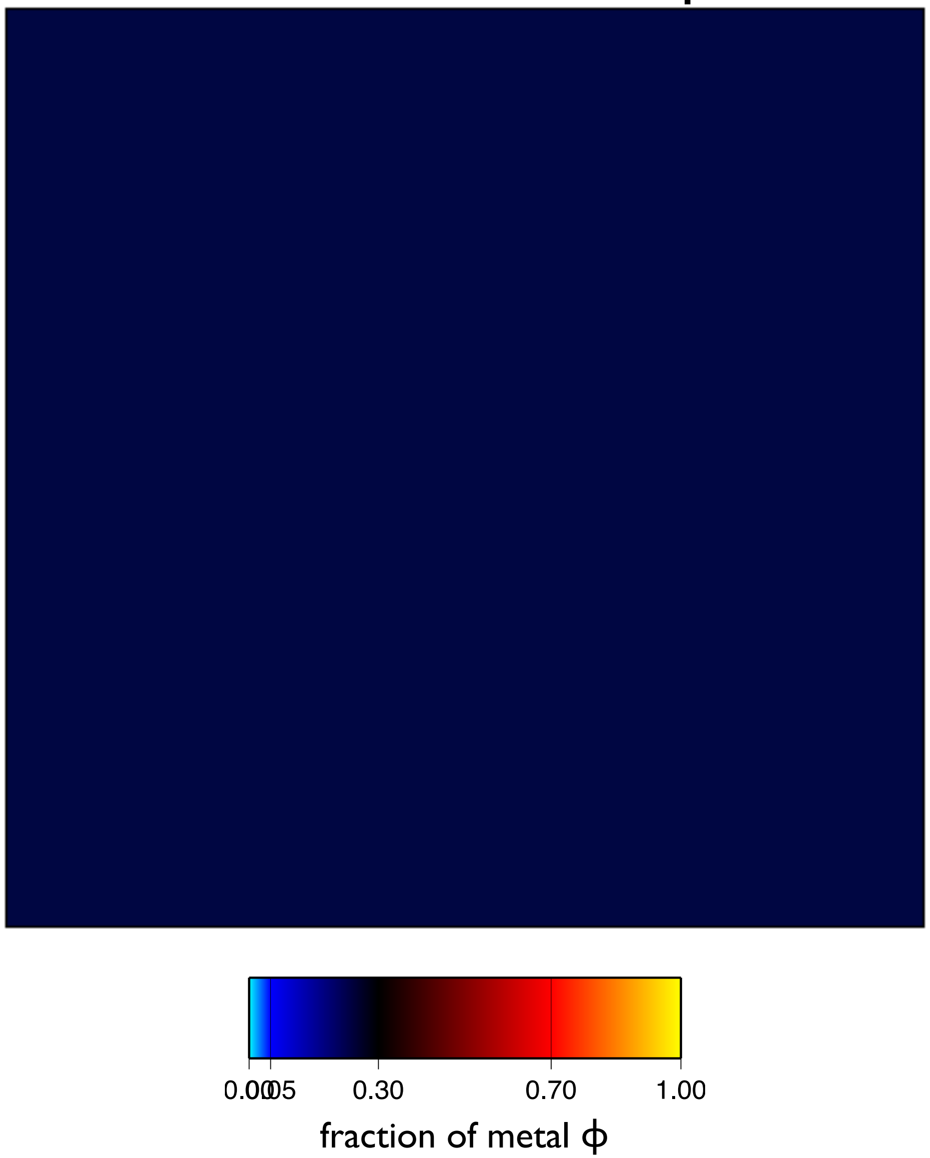

temperature T

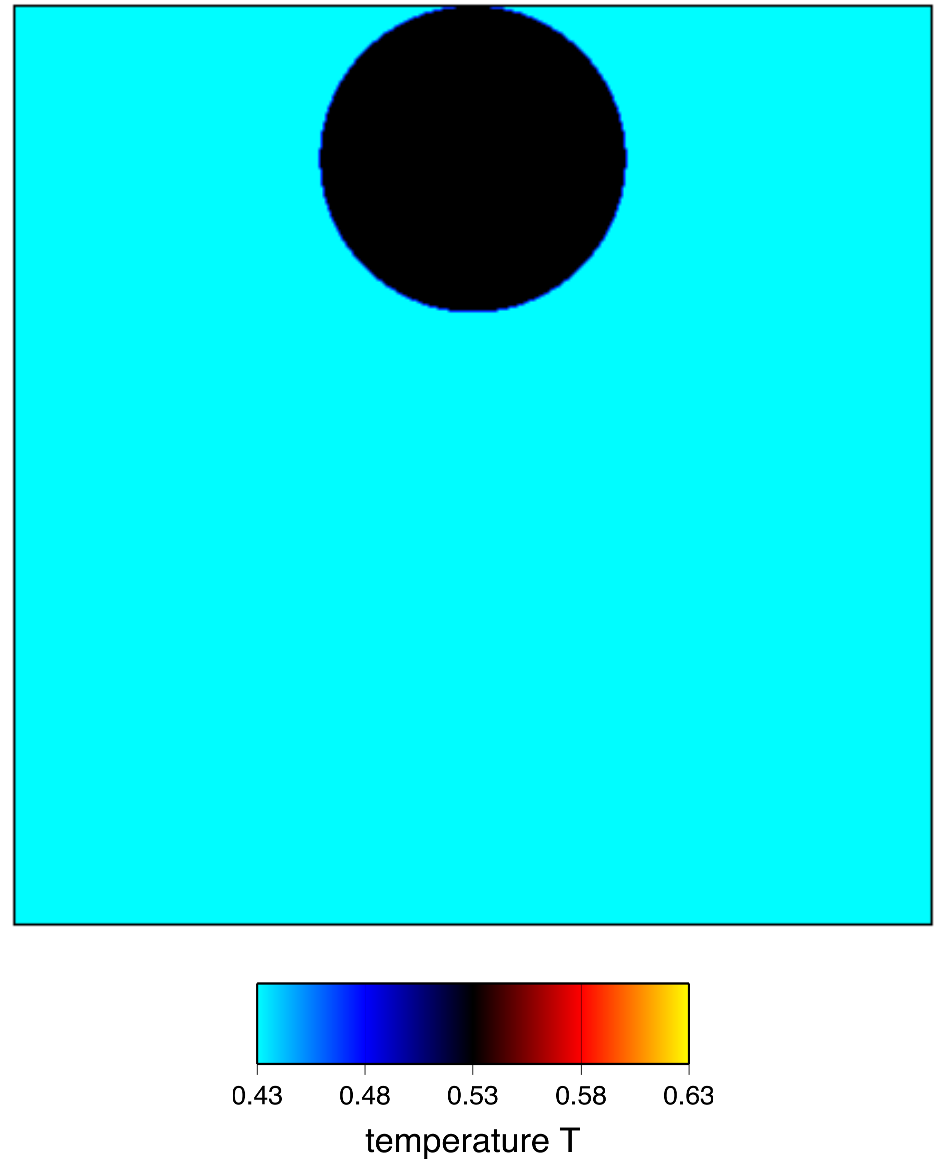

Ricard et al. (2009), Šrámek et al. (2010)

Simulation of an impact-induced differentiation

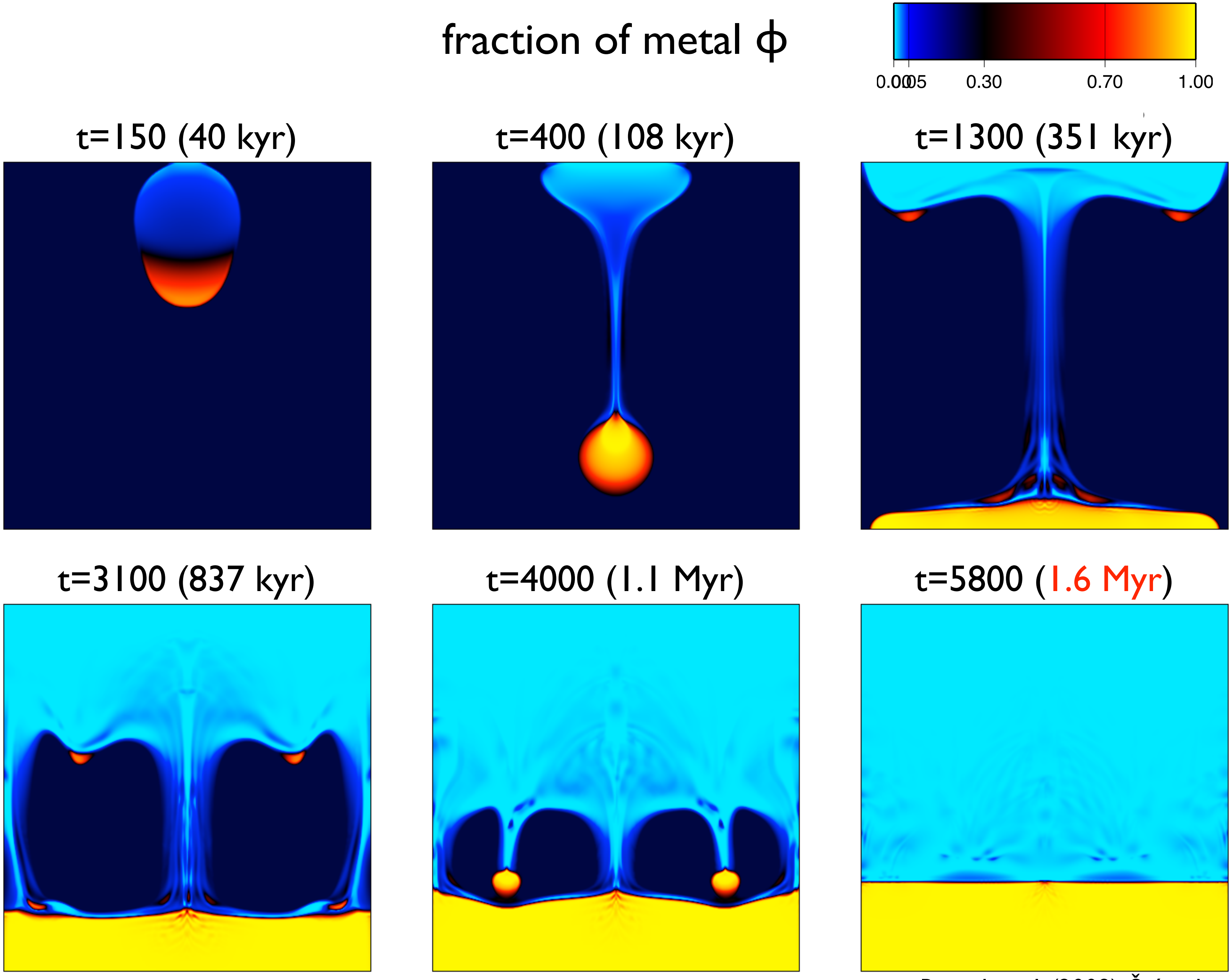

Ricard et al. (2009), Šrámek et al. (2010)

Simulation of an impact-induced differentiation

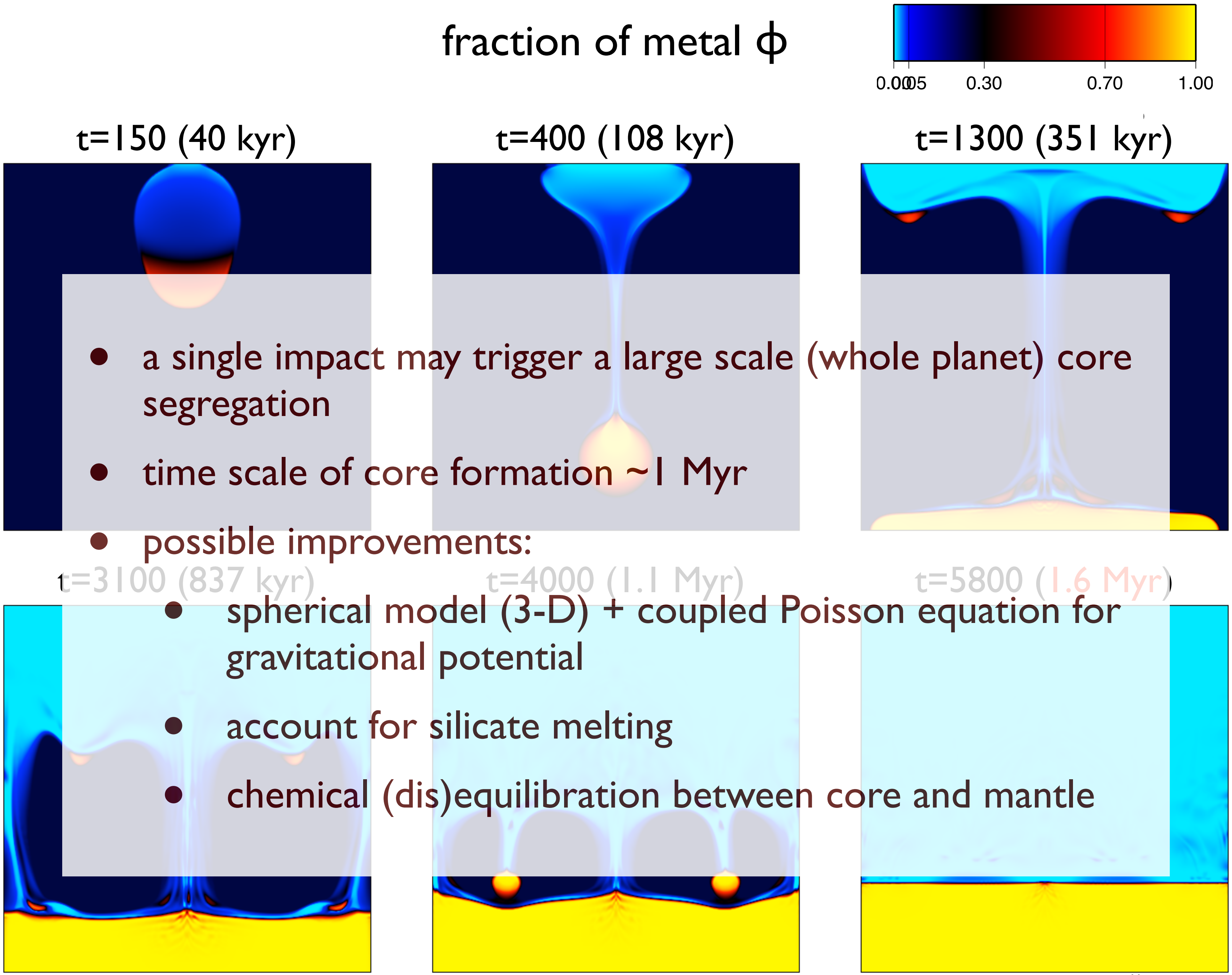

- a single impact may trigger a large scale (whole planet) core segregation
- time scale of core formation ~1 Myr
- possible improvements:
  - spherical model (3-D) + coupled Poisson equation for gravitational potential
  - account for silicate melting
  - chemical (dis)equilibration between core and mantle

Ricard et al. (2009), Šrámek et al. (2010)

Application II:
Coupling between compaction and melting

- aspect of partial melting below mid-ocean ridges
- equilibrium pressure release melting
- steady state, 1-D
- univariant melting (single component)
- solid matrix upwelling at a prescribed velocity V
- two-phase region between pure solid (ϕ=0) and pure melt (ϕ=1)

Does deformation affect melting?

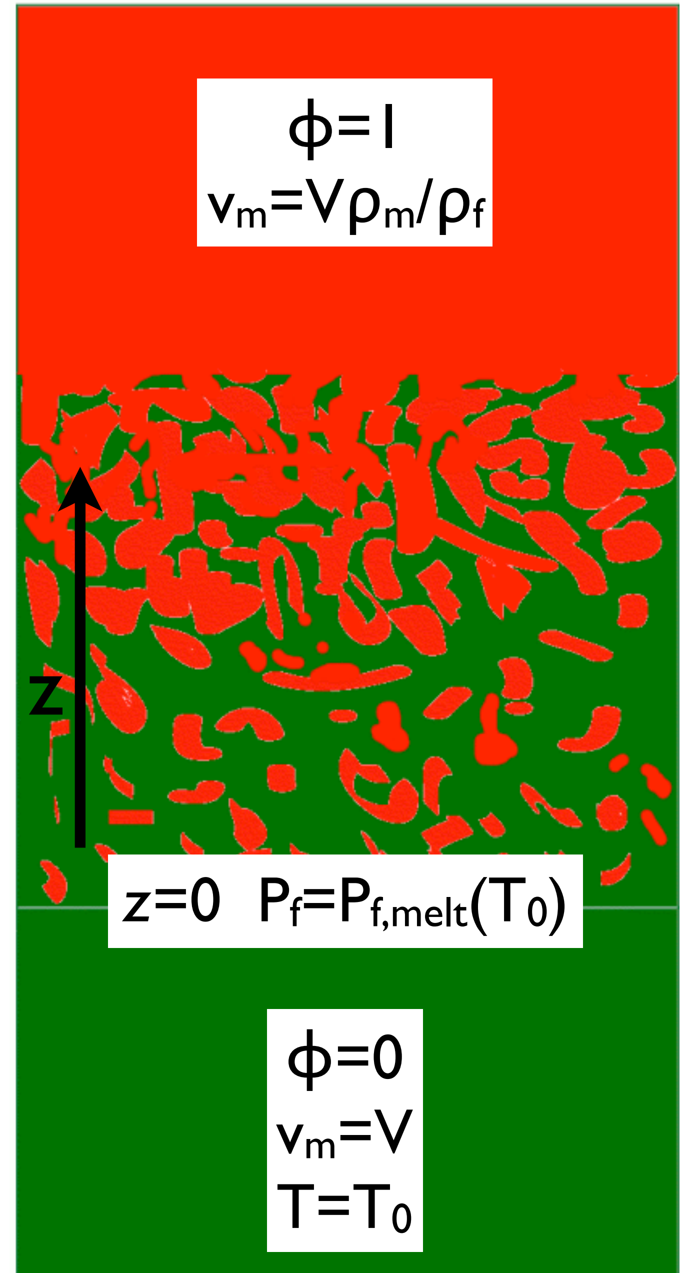

Force balance in the two-phase zone

$$\delta^2 \phi \frac{\mathrm{d}}{\mathrm{d}z}\left(\frac{1-\phi^2}{\phi}\frac{\mathrm{d}v_m}{\mathrm{d}z}\right) - \Delta v = V_B \phi (1-\phi)$$

matrix viscous forces — Darcy drag — buoyancy

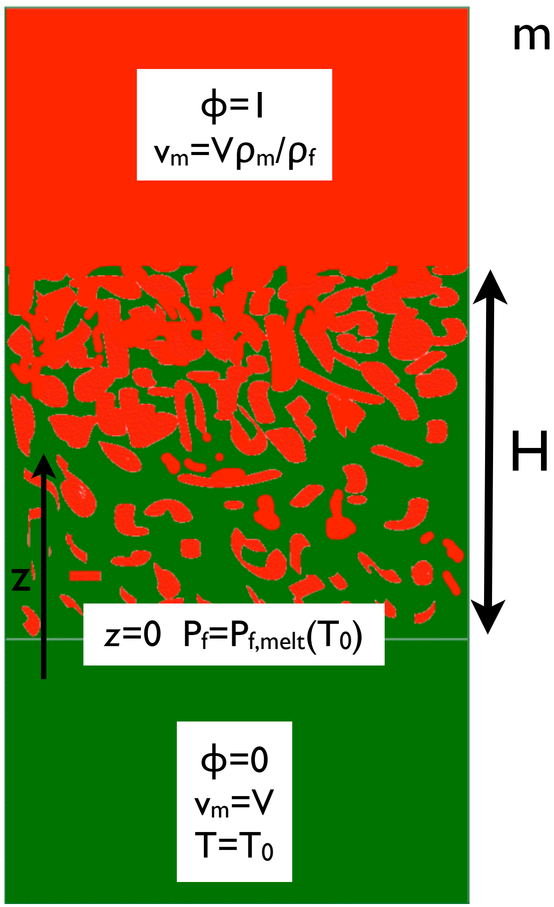

$$\delta^2 = \frac{4\mu_m}{3cH^2} = \frac{4\mu_m k_0}{3\mu_f H^2}$$

dimensionless compaction length δ

$$V_B = \frac{\Delta\rho g}{cV} = \frac{\Delta\rho g k_0}{\mu_f V}$$

dimensionless buoyancy velocity V_B

oceanic spreading center:

$\delta \sim 0.1$
$V_B \sim 100$

Darcy equilibrium (δ=0) – porosity

$$\delta^2\phi\frac{\mathrm{d}}{\mathrm{d}z}\left(\frac{1-\phi^2}{\phi}\frac{\mathrm{d}v_m}{\mathrm{d}z}\right)-\Delta v=V_B\phi(1-\phi)$$

matrix viscous forces

Darcy drag

buoyancy

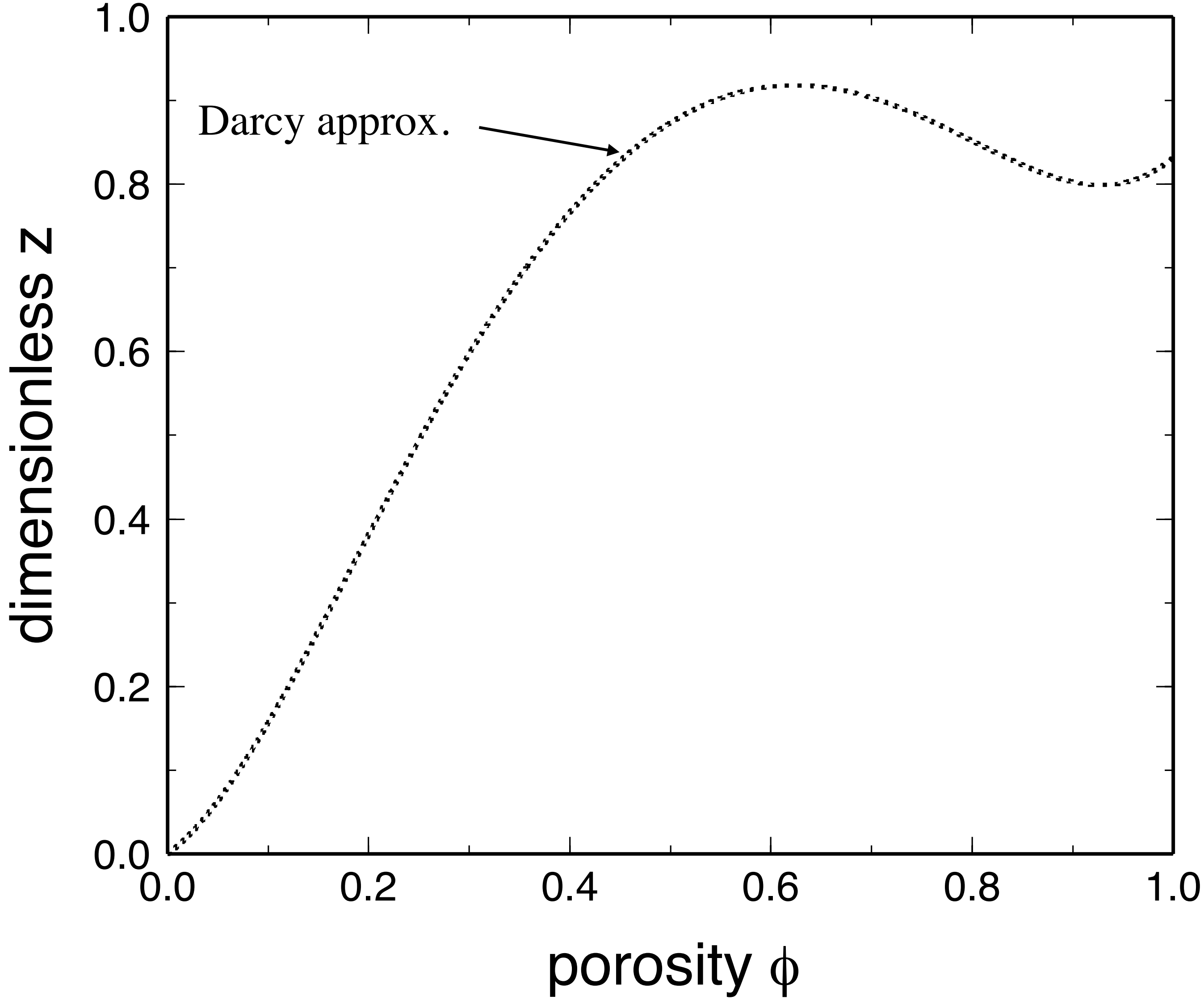

(δ=0.26, V_B=10)

Full solution – porosity

$$\delta^2 \phi \frac{\mathrm{d}}{\mathrm{d}z}\left(\frac{1-\phi^2}{\phi}\frac{\mathrm{d}v_m}{\mathrm{d}z}\right) - \Delta v = V_B \phi(1-\phi)$$

matrix viscous forces ↗ Darcy drag ↑ buoyancy ↖

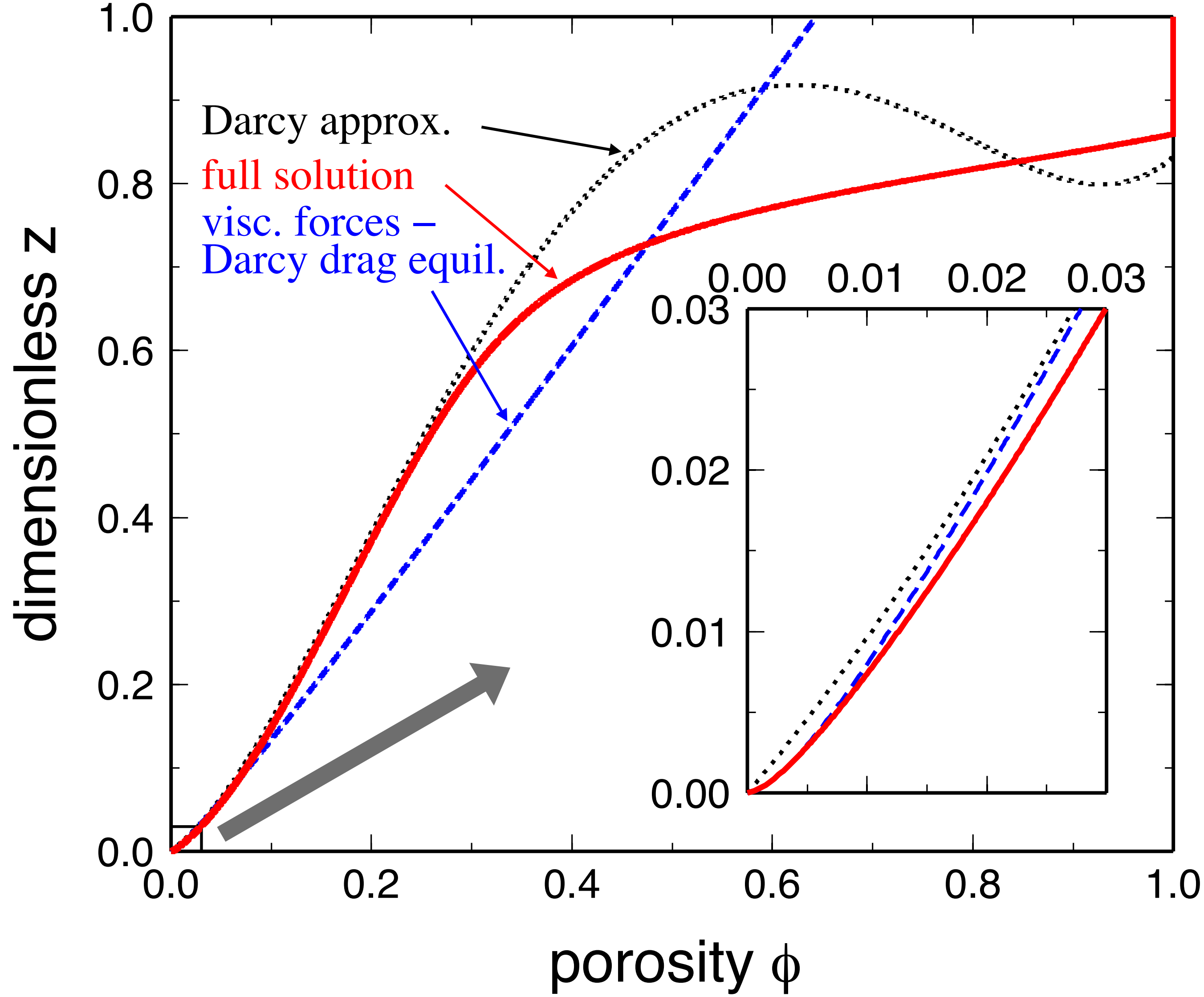

(δ=0.26, V_B=10)

Force balance in the partially molten region

$$\delta^2 \phi \frac{\mathrm{d}}{\mathrm{d}z}\left(\frac{1-\phi^2}{\phi}\frac{\mathrm{d}v_m}{\mathrm{d}z}\right) - \Delta v = V_B \phi (1-\phi)$$

matrix viscous forces ↗ Darcy drag ↑ buoyancy ↖

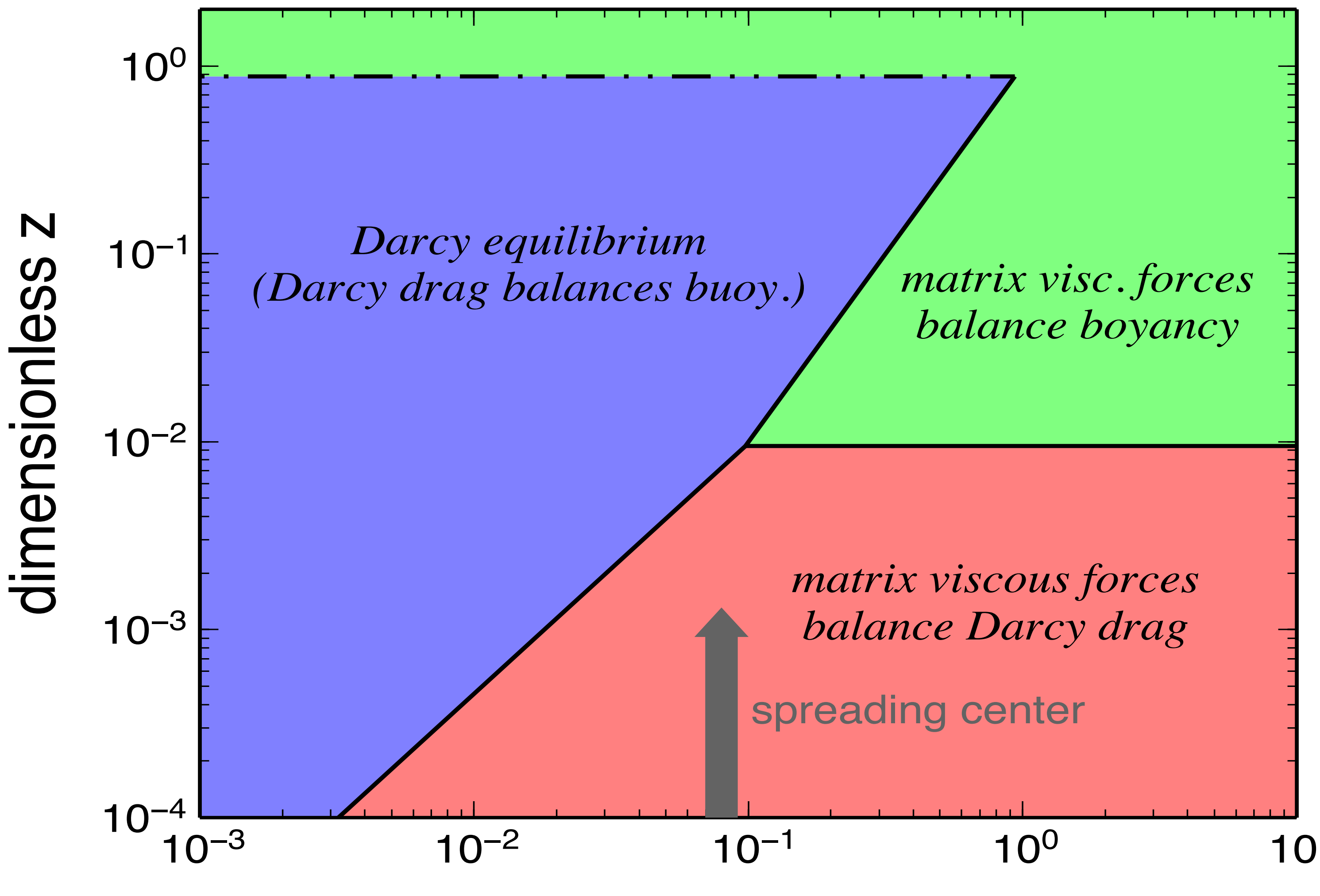

(V_B=60)

Šrámek et al. (2007)

Pressure difference between solid and melt – – Depth of incipient melting

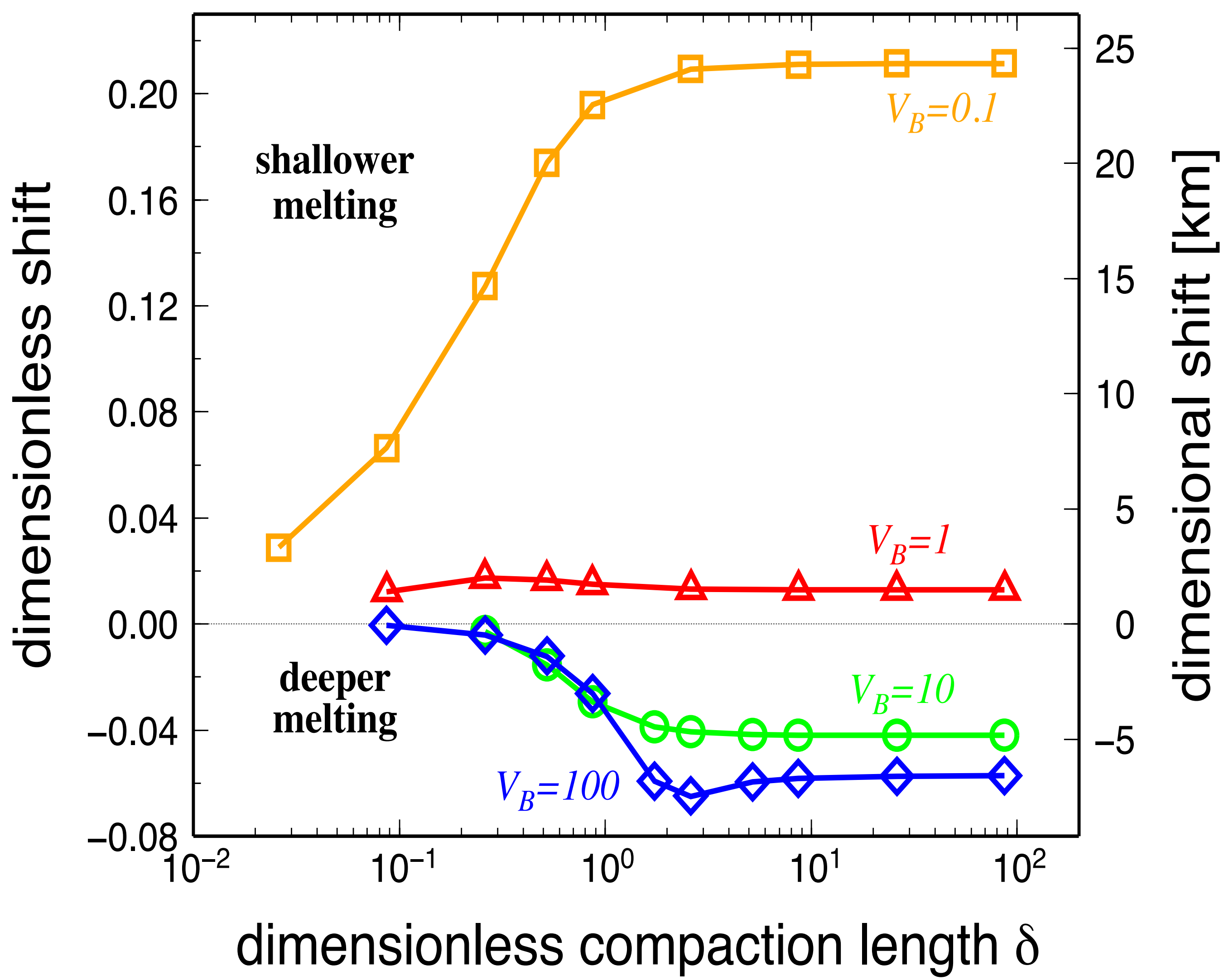

$V_B < 1$
inefficient melt extraction
matrix dilates, $P_f > P_m$
need lower average pressure, i.e., shallower depth to melt

$V_B > 1$
melt readily extracted
matrix compacts, $P_f < P_m$
can melt at higher average pressure, i.e. deeper

Melting begins at different depth than what predicts average pressure.

Šrámek et al. (2007)

Summary

- many geophysical problems involve multi-phase multi-component flow and deformation
- analysis and modeling of these complex media is becoming more common in geophysics and planetary physics
- leads to more complicated mathematical models relative to what most geodynamics typically deals with
- excellent opportunity for interaction between fields of geophysics, mathematical analysis, computational science

Metal–silicate differentiation

$$\Delta T_{impact} = \frac{4\pi}{3}\frac{f_1}{f_2}\frac{G\bar{\rho}R^2}{C}$$

Monteux et al. (2007)

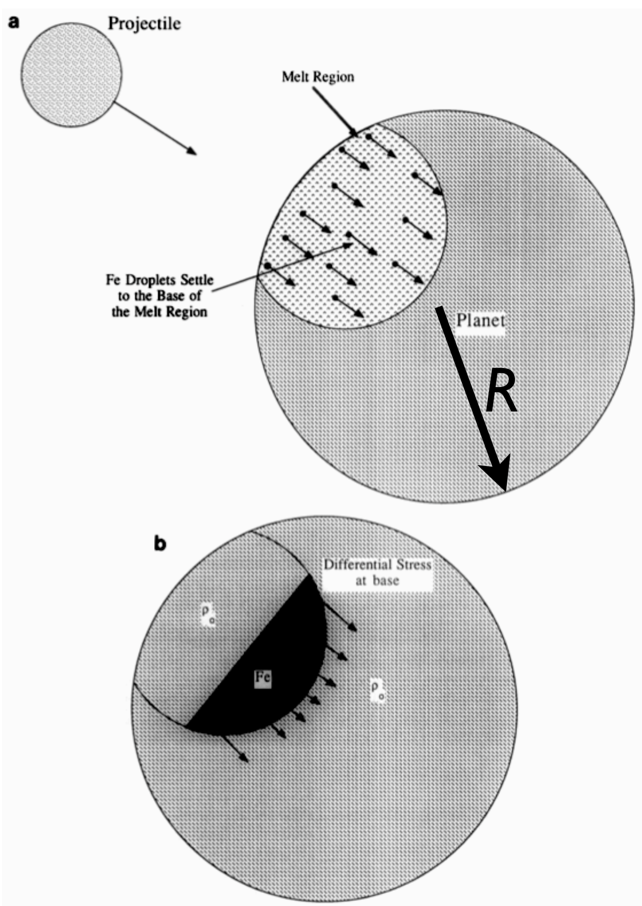

Tonks & Melosh (1992)

- metal is ~2x denser than silicate
- initial undifferentiated state
- impact heating
- metal can melt
- then it can easily sink through the silicates
- gravitational energy is released as heat
- more metal melts
- runaway instability??

regime diagram

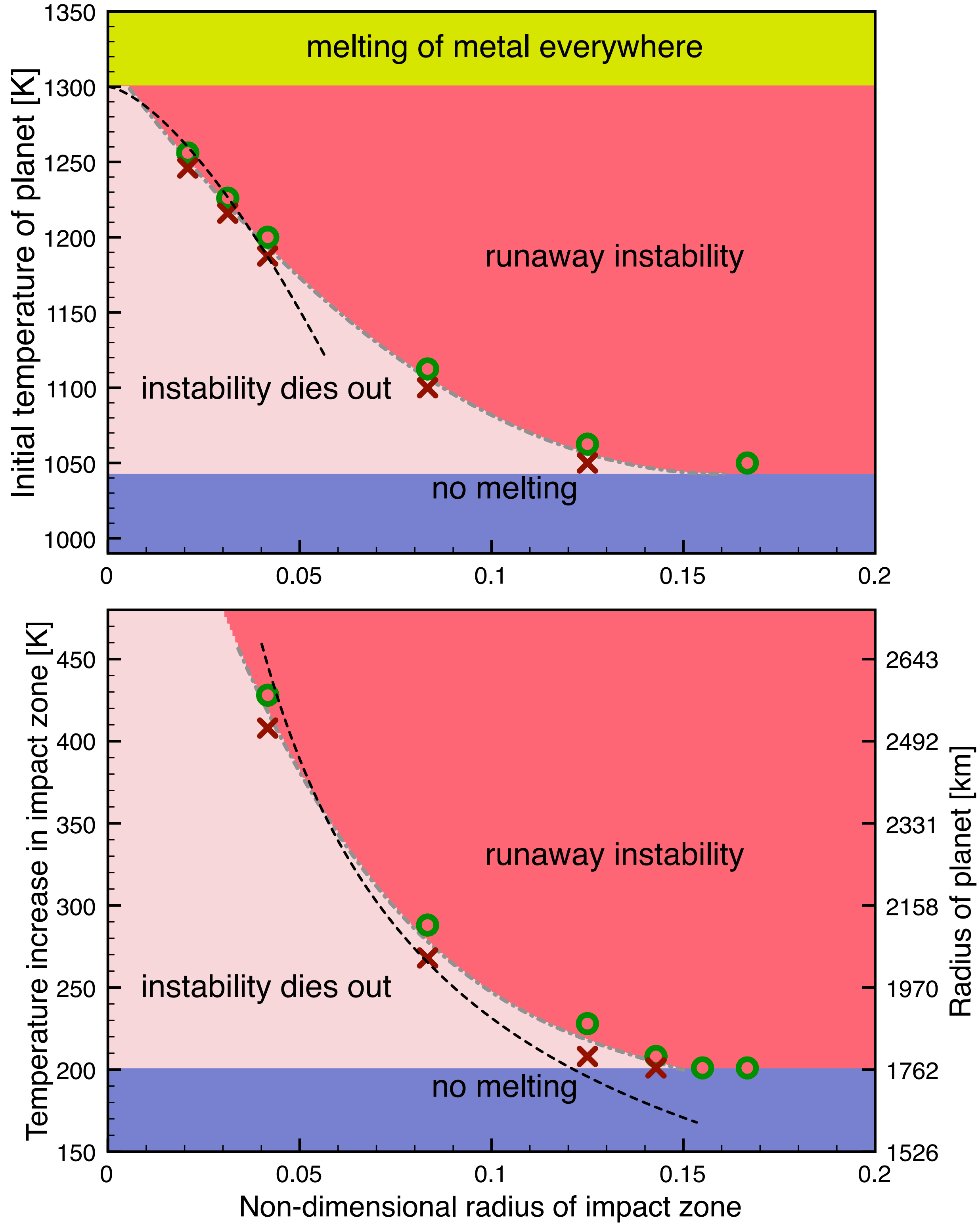

Thermal evolution and differentiation of growing planetesimal

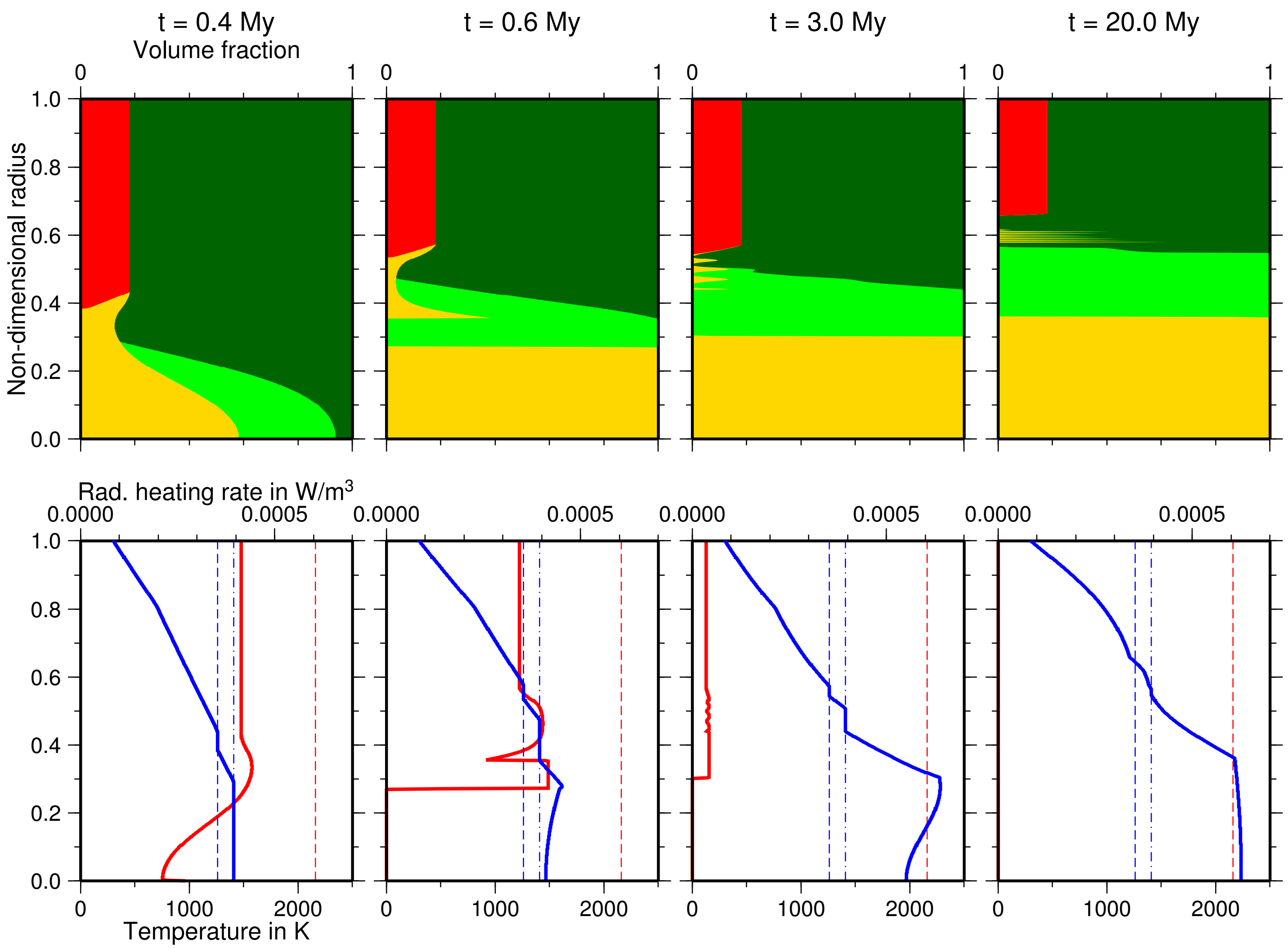

R = 500 km, t_{acc} = 3 My, β = 0

Thermal evolution and differentiation of growing planetesimal

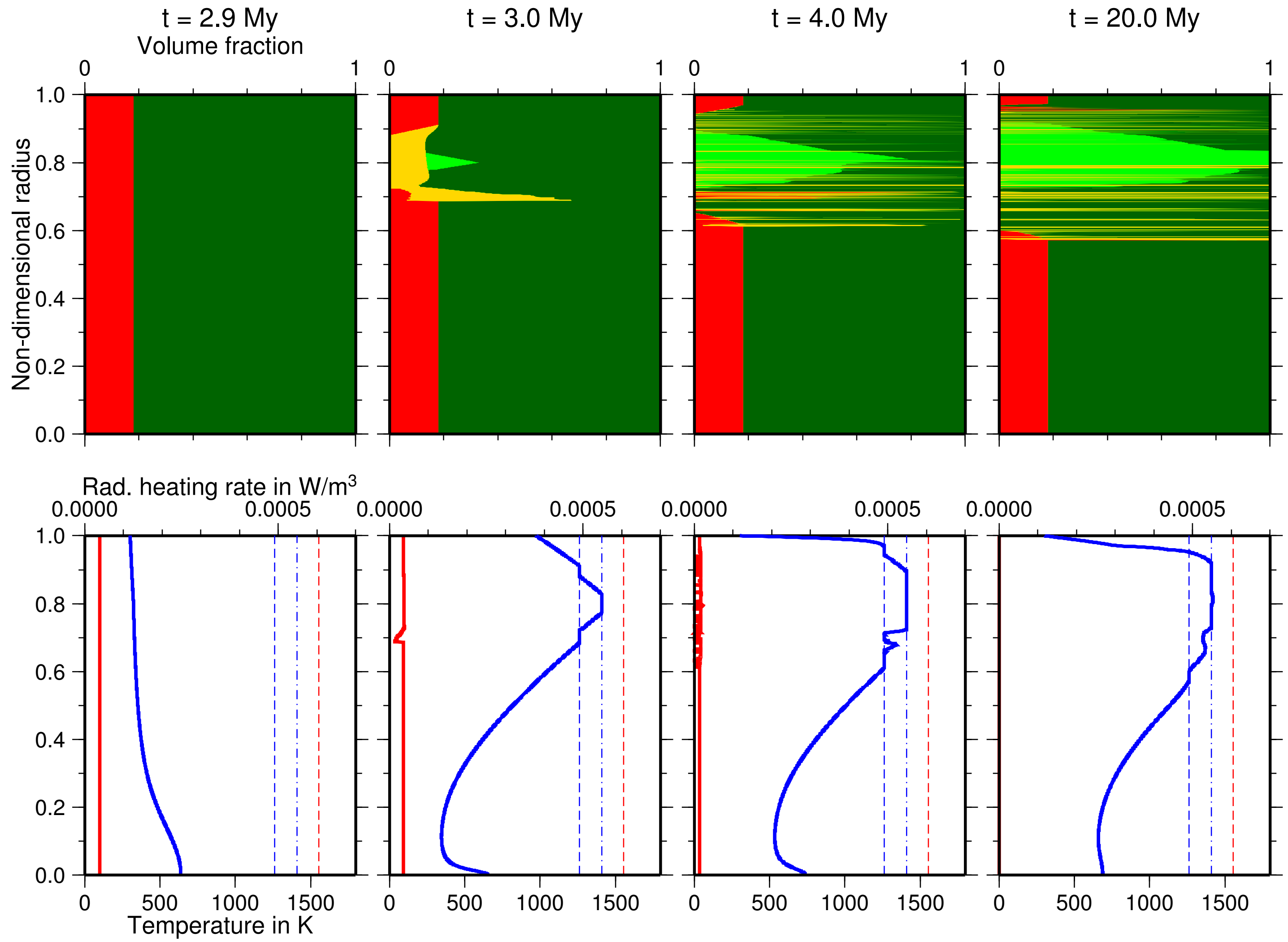

R = 1500 km, t_{acc} = 3 My, $\beta = 2$

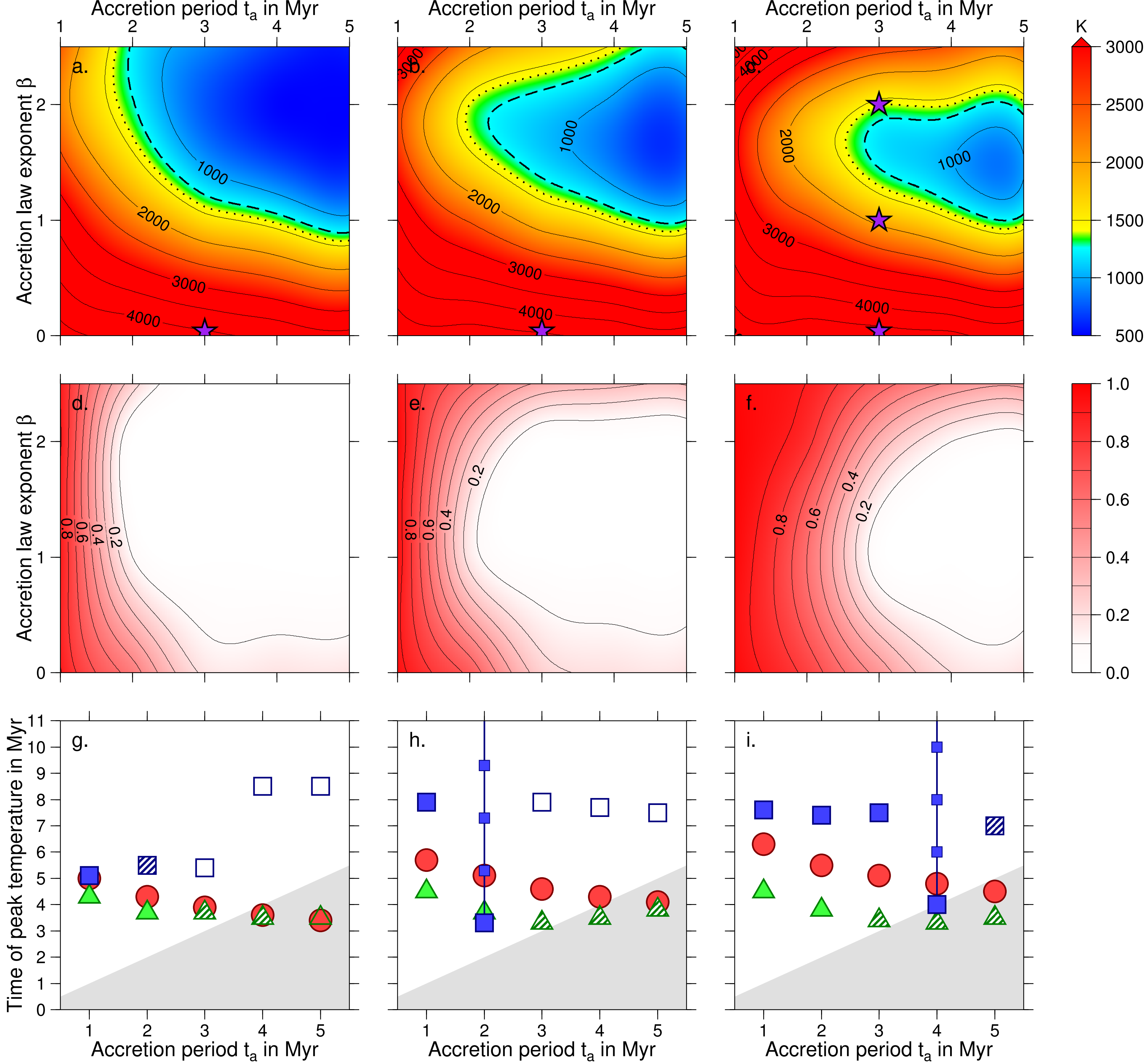

Accretion period t_a in Myr
Accretion law exponent β
Time of peak temperature in Myr
K
a.
b.
c.
d.
e.
f.
g.
h.
i.
1000
2000
3000
4000
0.2
0.4
0.6
0.8
3000
2500
2000
1500
1000
500
1.0
0.8
0.6
0.4
0.2
0.0

Core formation
Hot topic in geophysics

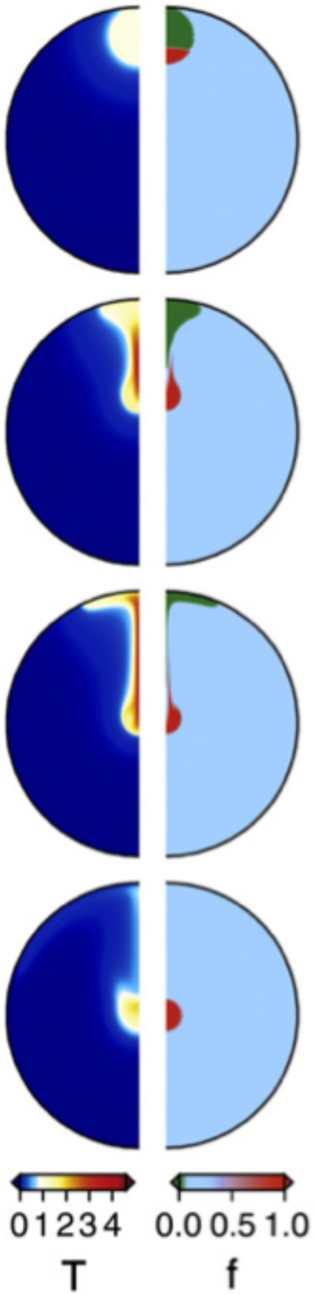

Monteux et al. (2009)

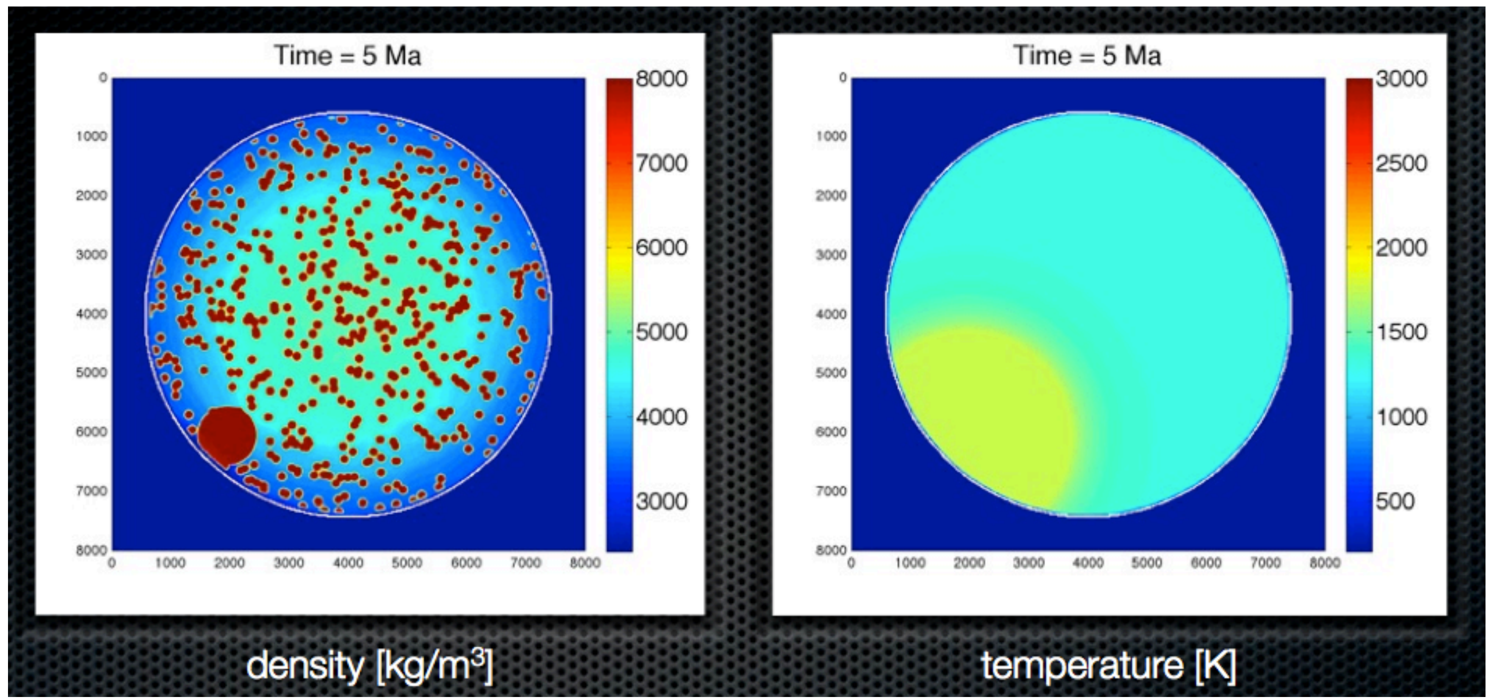

Golabek et al. (2010)

these are not two-phase models

Melt generation, focusing and extraction below mid-ocean ridge

2 phases
+ chem. components

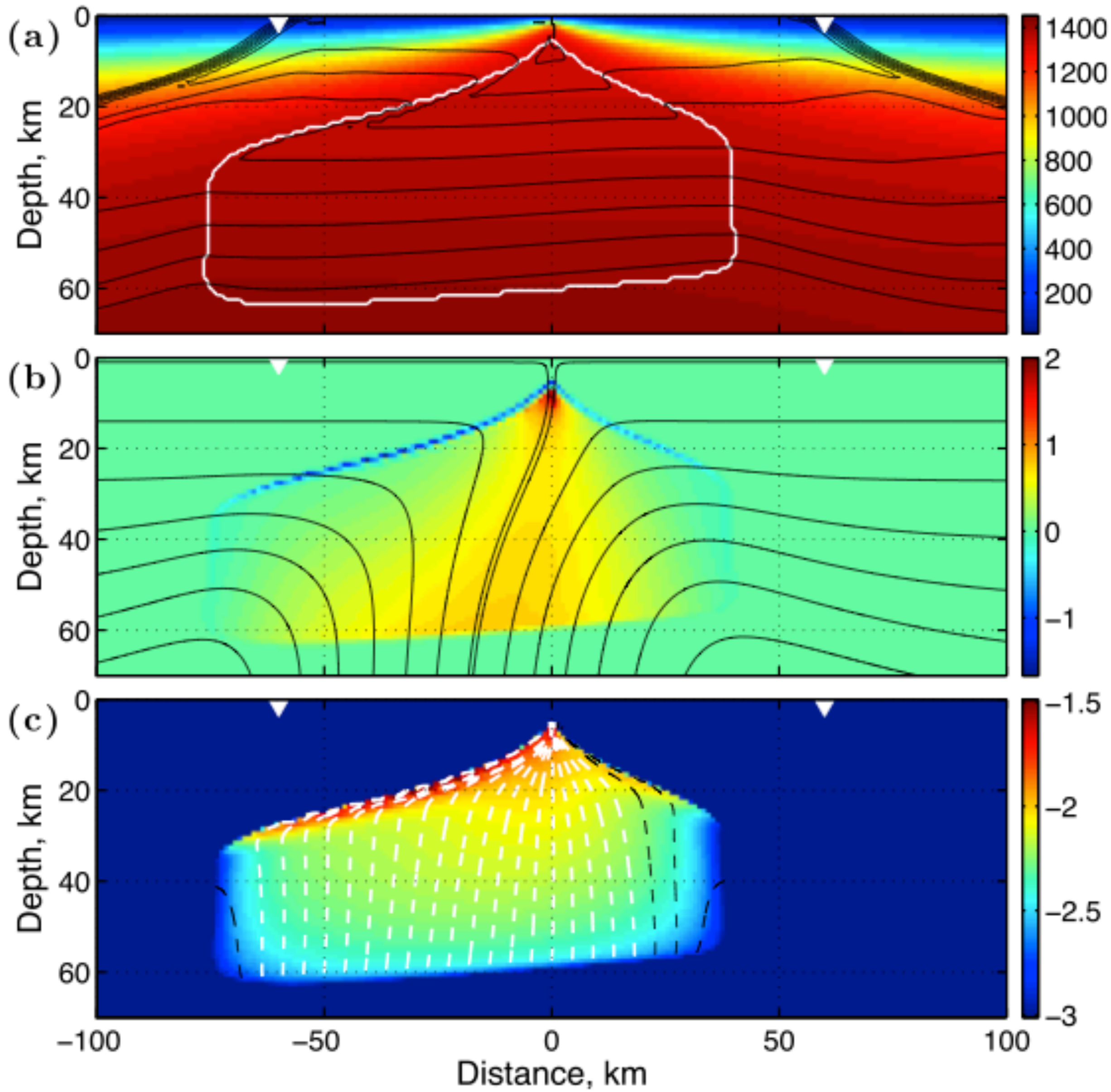

Temperature (color)
Melt fraction (contours)

Melting rate (color)
Solid streamlines

$\log_{10}$(porosity)
Magma streamlines

Katz (2010)

Porosity and velocities

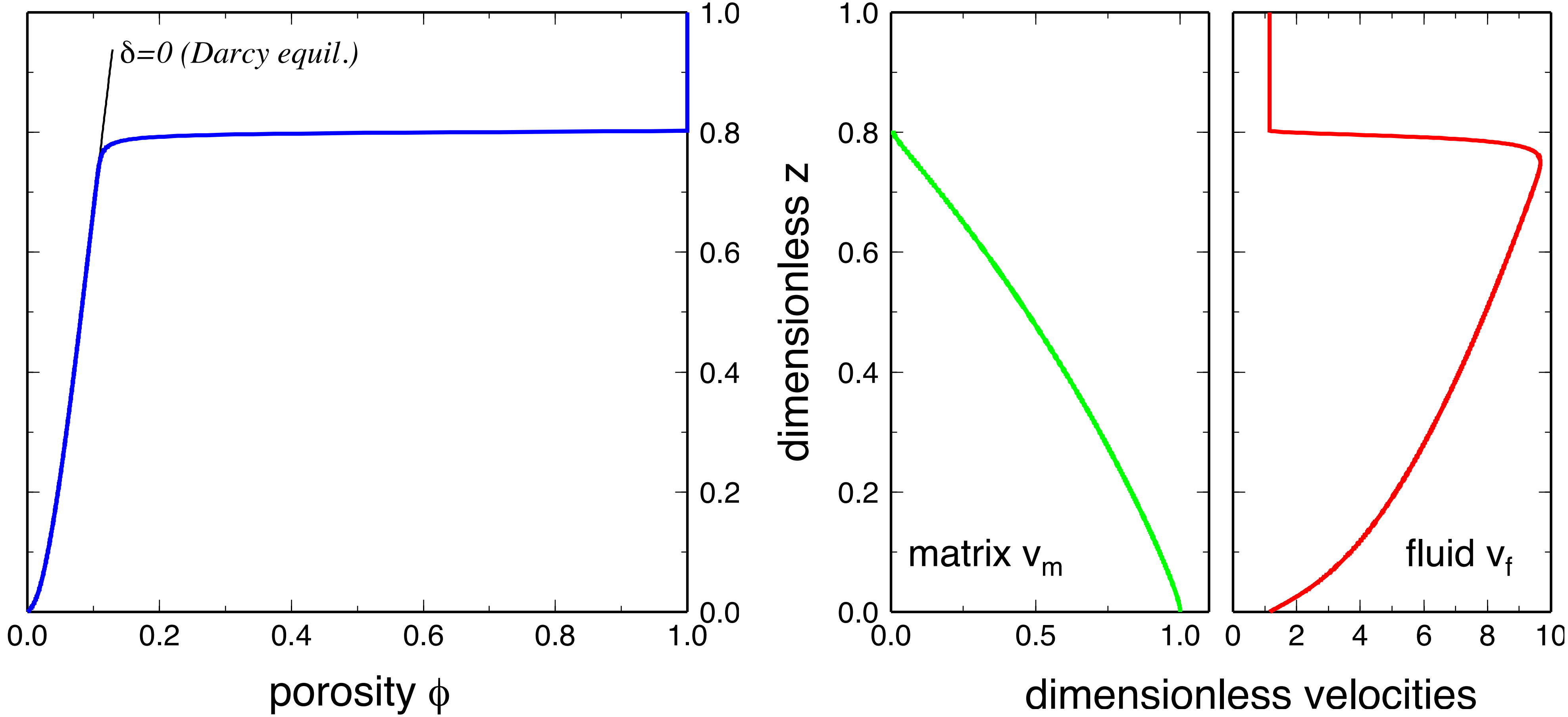

(δ=0.26, V_B=100)

Physics of two-phase flow

I. Interconnectivity

dihedral angle ... crude assessment of interconnectivity

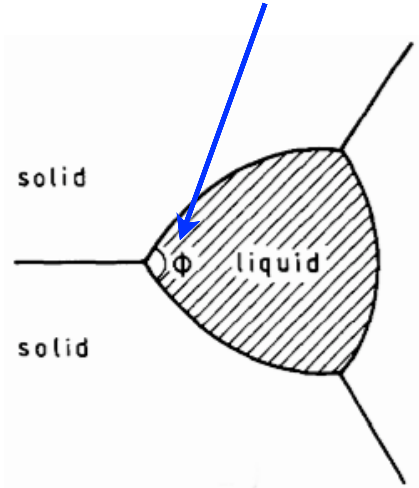

depends on the ratio of solid–solid and solid–liquid interfacial energies

< 60°
interconnected network

> 60°
isolated pockets of liquid

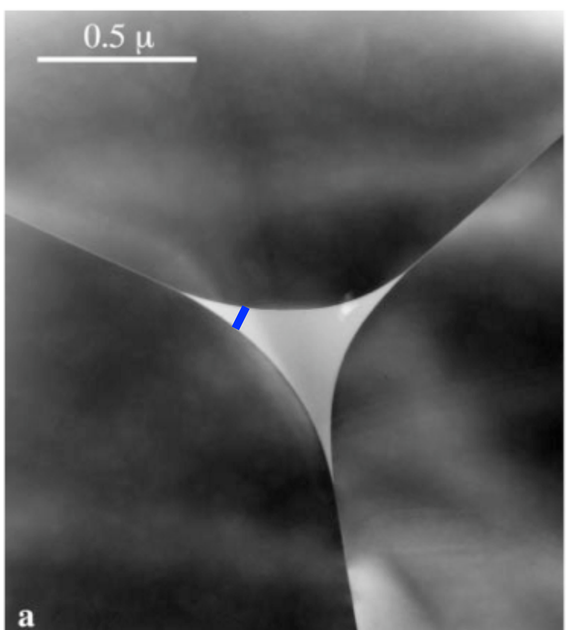

Cmíral et al. (1998)

after Schmeling (1985)

Physics of two-phase flow

1. Interconnectivity

partial melting in the upper mantle
basaltic magma and olivine matrix

- dihedral angle 20°– 50°
- interconnected at low melt fraction

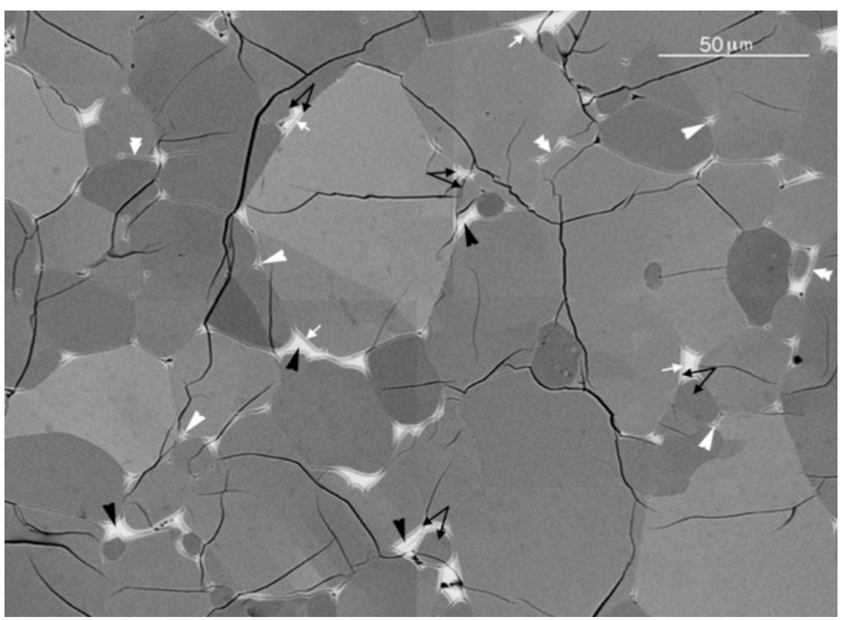

Cmíral et al. (1998)

metal–silicate differentiation
molten iron alloy and silicate matrix

- dihedral angle probably >60°
- interconnectivity threshold ~ 5% of metal

4% FeS melt   6% FeS melt

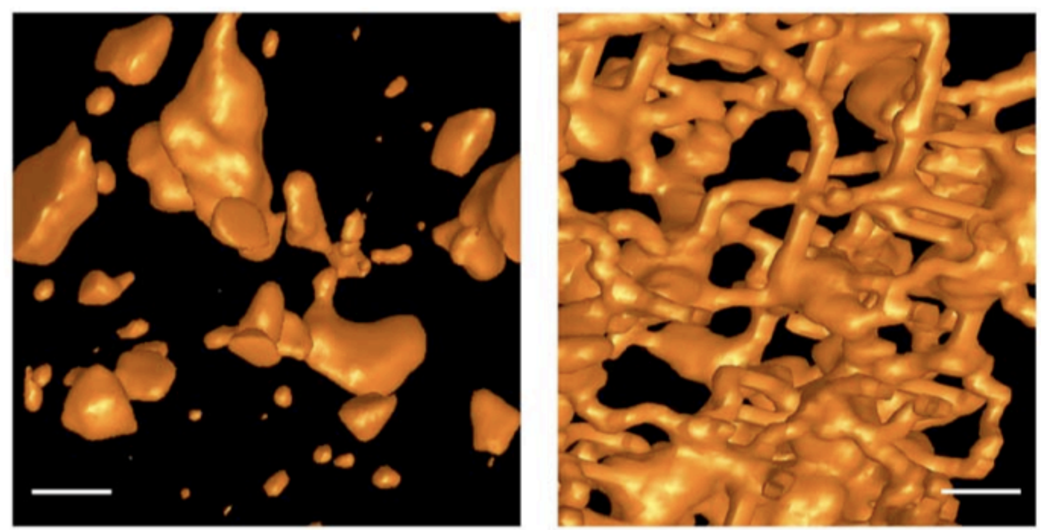

Roberts et al. (2007)

Physics of two-phase flow

2. Permeability and Darcy's law

matrix permeability

$$\mathbf{v}_D = -\frac{k}{\mu}\nabla P$$

Darcy velocity

fluid viscosity

- geometric representation of interconnected fluid network
- solve Poiseuille flow
- get permeability k

$$k(\phi) = \frac{b^2\phi^n}{a} = k_0\phi^n$$

- ϕ porosity
- *n* typically 2 or 3
- *a* ~ 100–1000 "tortuosity"

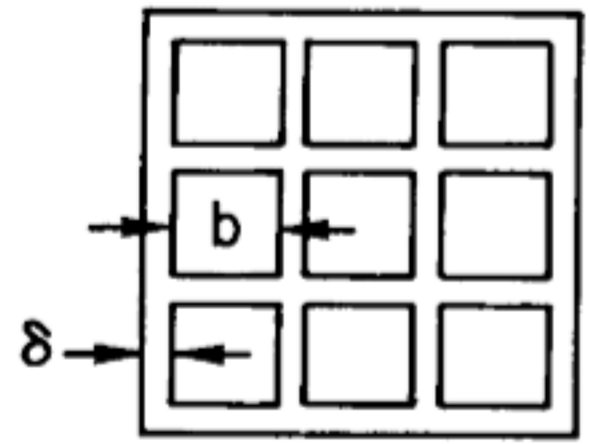

Ahern & Turcotte (1979)

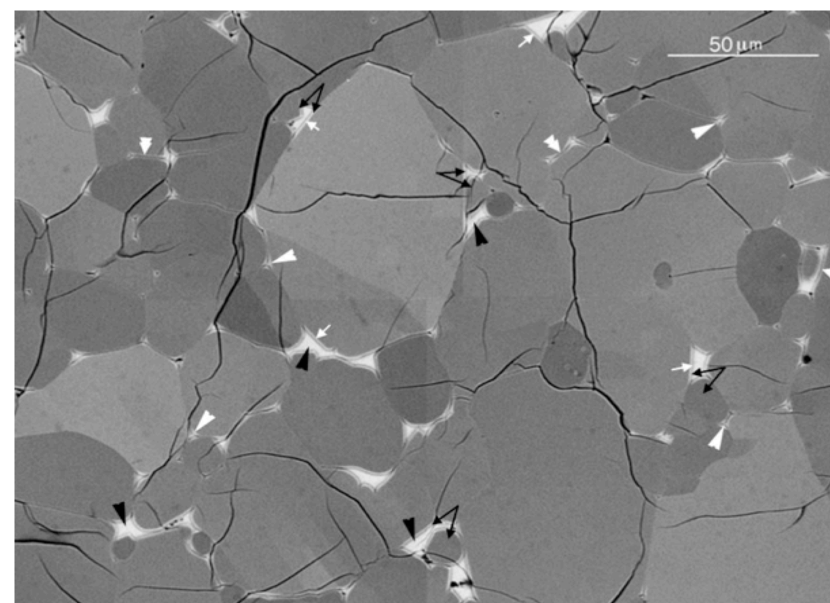

Cmíral et al. (1998)

Non-equilibrium thermodynamics

relation for pressure difference

$\frac{\mathrm{d}\alpha}{\mathrm{d}\phi}$ sum of principal interface curvatures

$$\Delta P + \sigma \frac{\mathrm{d}\alpha}{\mathrm{d}\phi} = -\frac{K_0 \mu_m}{\phi} \nabla \cdot \mathbf{v}_m$$

deviation of pressure difference from the static Laplace's condition $\propto$ compaction/dilation of the matrix

kinetic relation for melting rate

$$\Delta\Gamma = \chi \left(\Delta\varepsilon - T\Delta s - P_f \frac{\Delta\rho}{\rho_f \rho_m} - \frac{\sigma}{\rho_m} \frac{\mathrm{d}\alpha}{\mathrm{d}\phi} \right)$$

melting rate $\propto$ departure from equilibrium

Equilibrium melting temperature

$$T = T_0 + \gamma \overline{P} - \frac{\sigma}{\Delta s} \frac{\overline{\rho}}{\rho_f \rho_m} \frac{\mathrm{d}\alpha}{\mathrm{d}\phi} + \gamma K_0 \mu_m \frac{1-\phi}{\phi} \nabla \cdot \mathbf{v}_m$$

the "classical" Clapeyron slope is modified by surface tension and matrix compaction/dilation

Parameters – model of partial melting

Table 6.1: Table of parameters applicable to dry melting below mid ocean spreading centers.

symbol	description	definition	possible ranges	preferred value	units
μ_f	fluid shear viscosity			10	Pa s
μ_m	matrix shear viscosity		10^{18}–10^{19}	10^{18}	Pa s
k_0	constant in permeability relationship		10^{-10}–10^{-9}	5×10^{-10}	m^2
c	Darcy interaction coefficient	μ_f / k_0	10^{10}–10^{11}	2×10^{10}	$Pa\,s\,m^{-2}$
ρ_f	fluid density			2800	$kg\,m^{-3}$
ρ_m	matrix density			3200	$kg\,m^{-3}$
g	gravitational acceleration			9.8	$m\,s^{-2}$
Δs	entropy of fusion	$s_m - s_f$	-(250–400)	-340	$J\,K^{-1}\,kg^{-1}$
C	heat capacity		1000–1300	1200	$J\,K^{-1}\,kg^{-1}$
T_0	initial temperature of upwelling		1573–1673	1673	K
V	initial velocity of upwelling		4–10	10	$cm\,yr^{-1}$
H	length scale	$\rho_f T_0 \Delta s^2 / (\Delta\rho g C)$	60–150	115	km
k'_T	thermal conductivity			3.7	$W\,m^{-1}\,K^{-1}$
k_T	dimensionless thermal conductivity	$\rho_f k'_T T_0 / (\rho_m \Delta\rho g V H^2)$		0.03	–
γ'	Clapeyron slope	$\Delta\rho / (\rho_f \rho_m \Delta s)$	100-133	130	$K\,GPa^{-1}$
γ	dimensionless Clapeyron slope	$\gamma' \rho_m g H / T_0 = -\Delta s / C$		0.28	–
δ'	compaction length	$\sqrt{4\mu_m/(3c)}$	8–26	8	km
δ	dimensionless compaction length	δ'/H	0.07–0.23	0.07	–
V_B	buoyancy velocity scale	$\Delta\rho g / (cV)$	60–1000	60	–
R	density ratio	ρ_f / ρ_m		0.875	–

Porosity and degree of melting

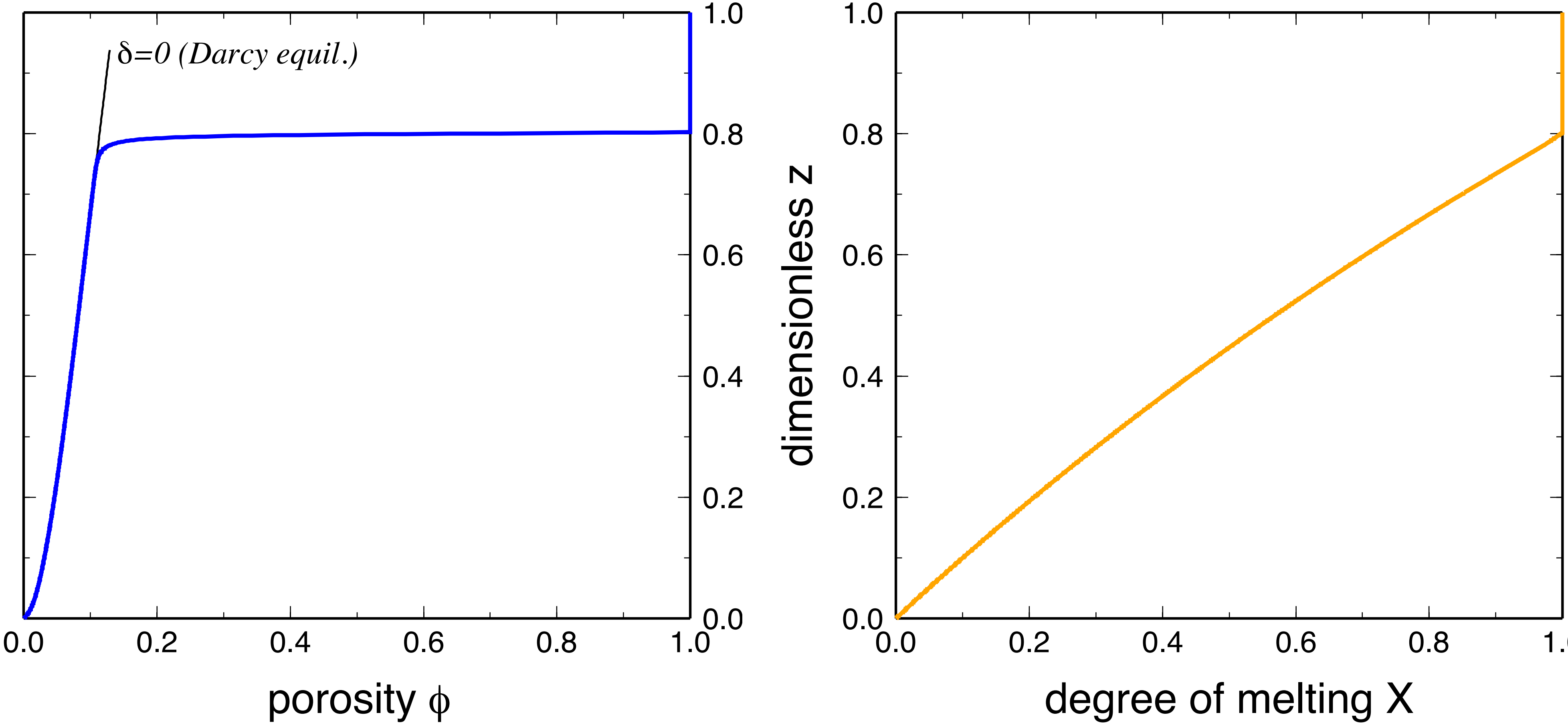

(δ=0.26, V_B=100)

Porosity and velocities

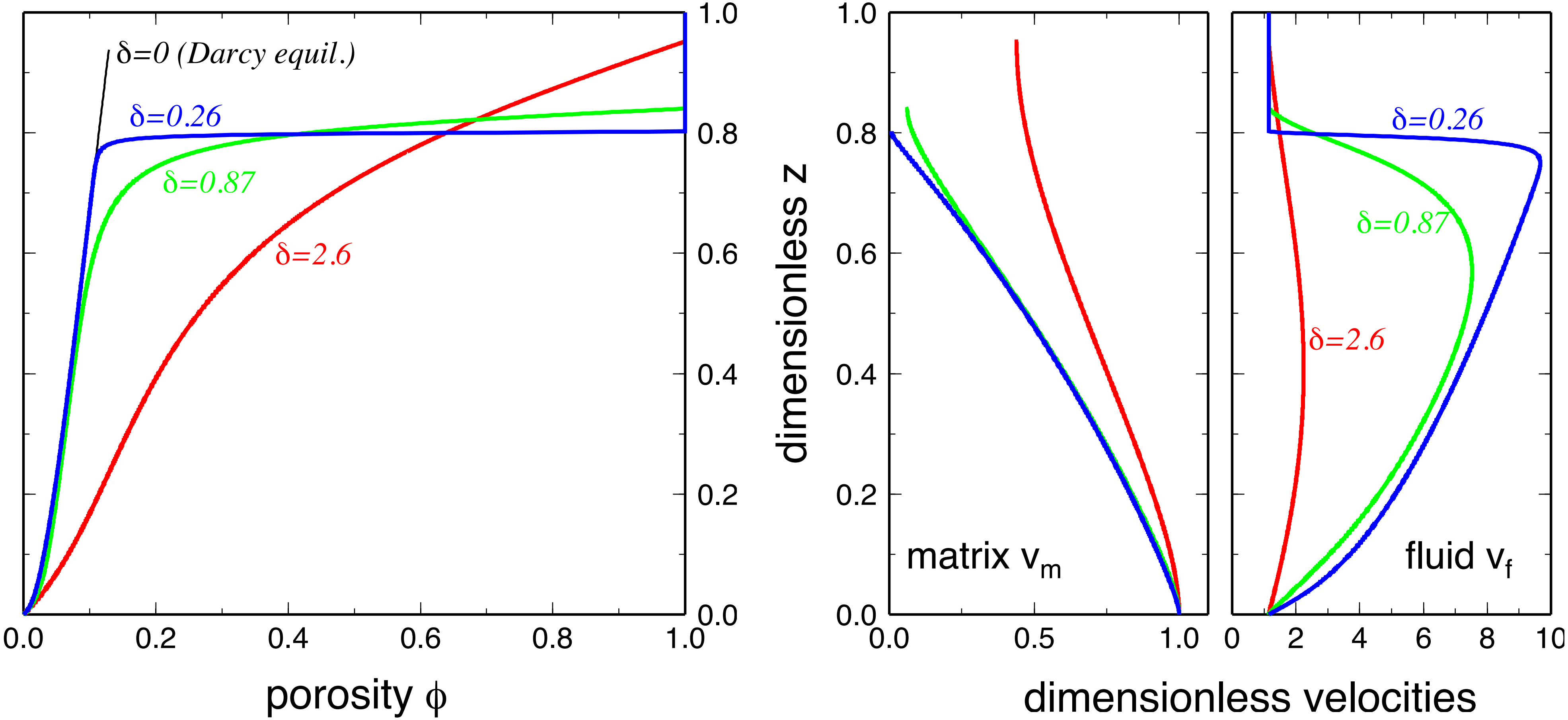

(V_B=100)

Porosity and degree of melting

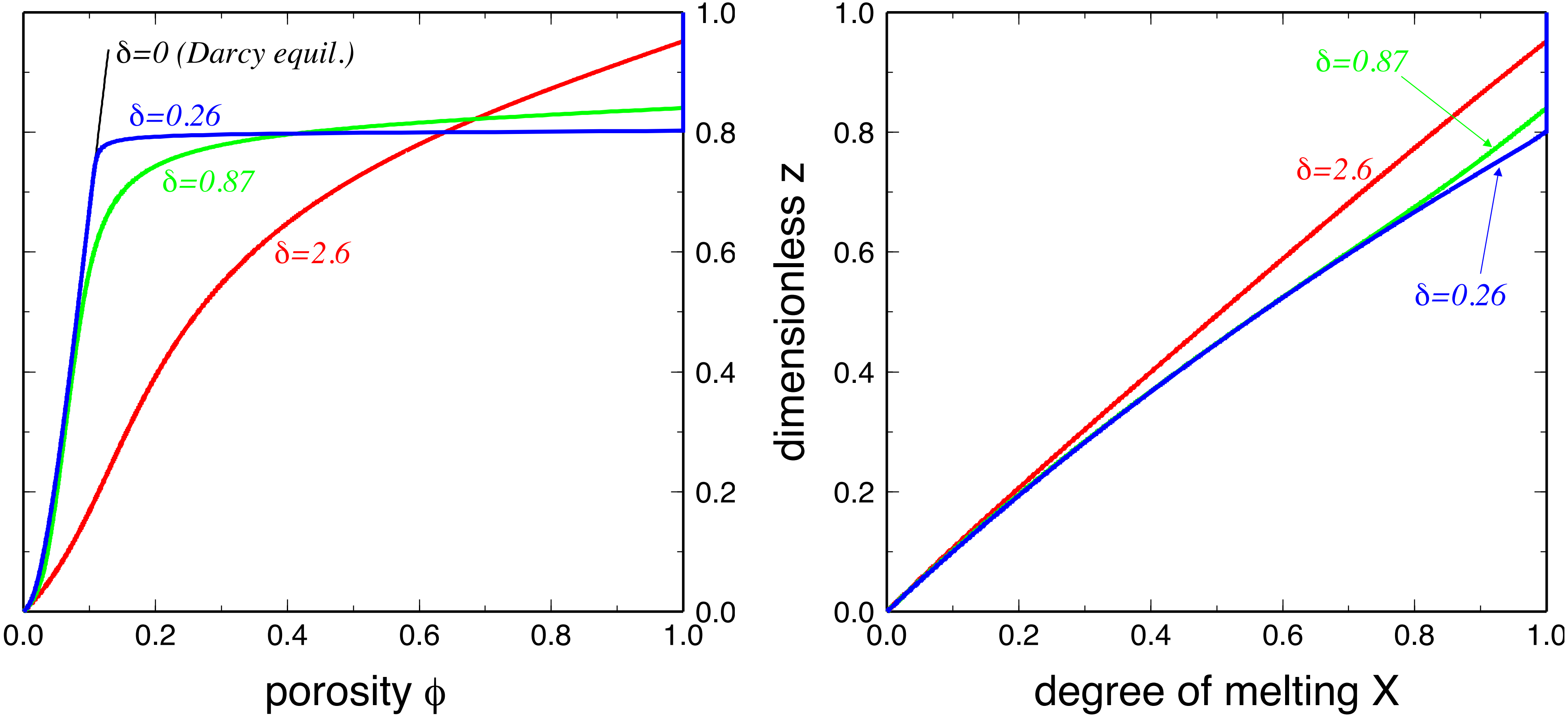

(V_B=100)

Melting rate and degree of melting

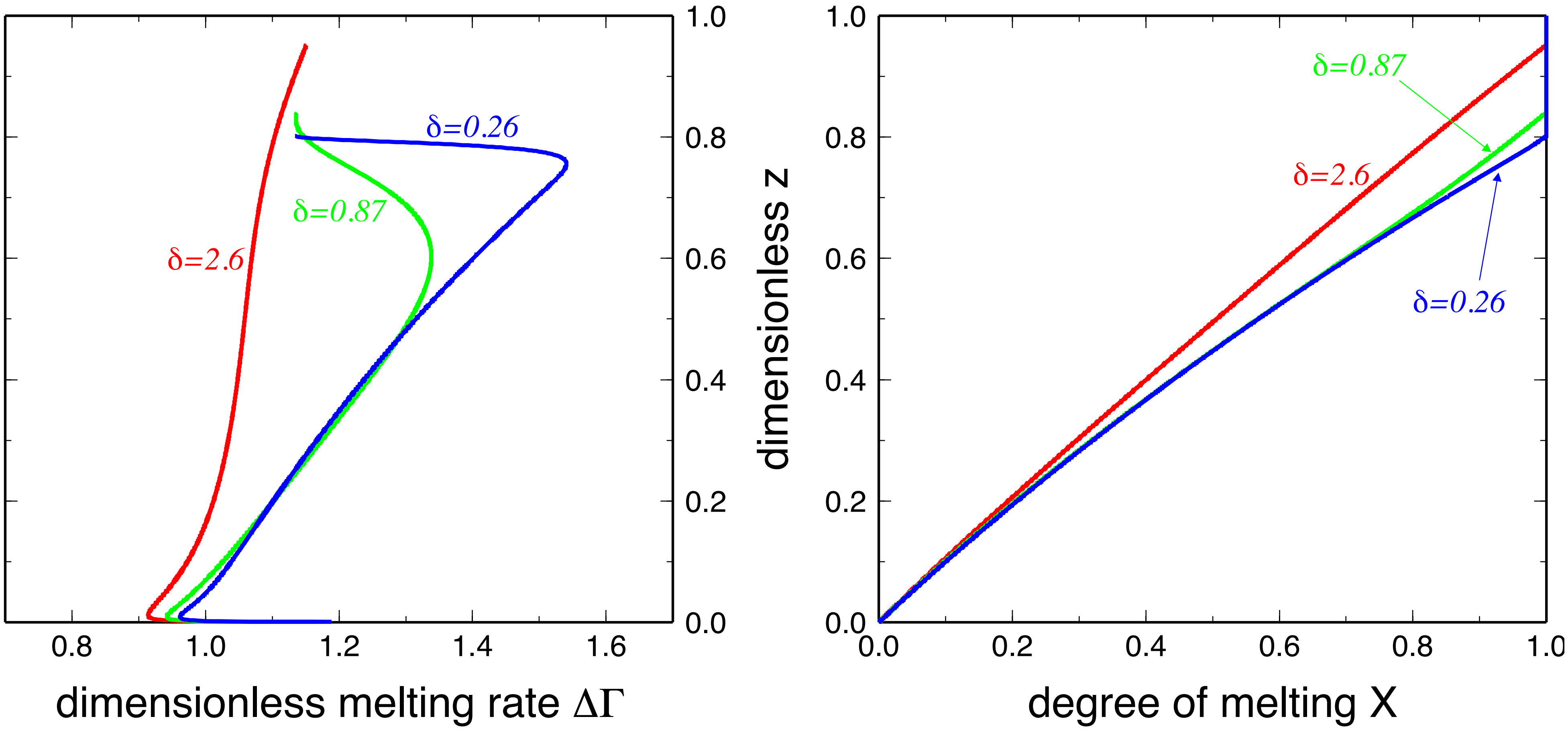

(V_B=100)

Full solution – pressure difference

$$\Delta P + \sigma \frac{\mathrm{d}\alpha}{\mathrm{d}\phi} = -\frac{K_0 \mu_m}{\phi} \nabla \cdot \mathbf{v}_m \xrightarrow{\sigma=0,\ 1\text{-D}} \Delta P = P_m - P_f = -\frac{K_0 \mu_m}{\phi} \frac{\mathrm{d}v_m}{\mathrm{d}z}$$

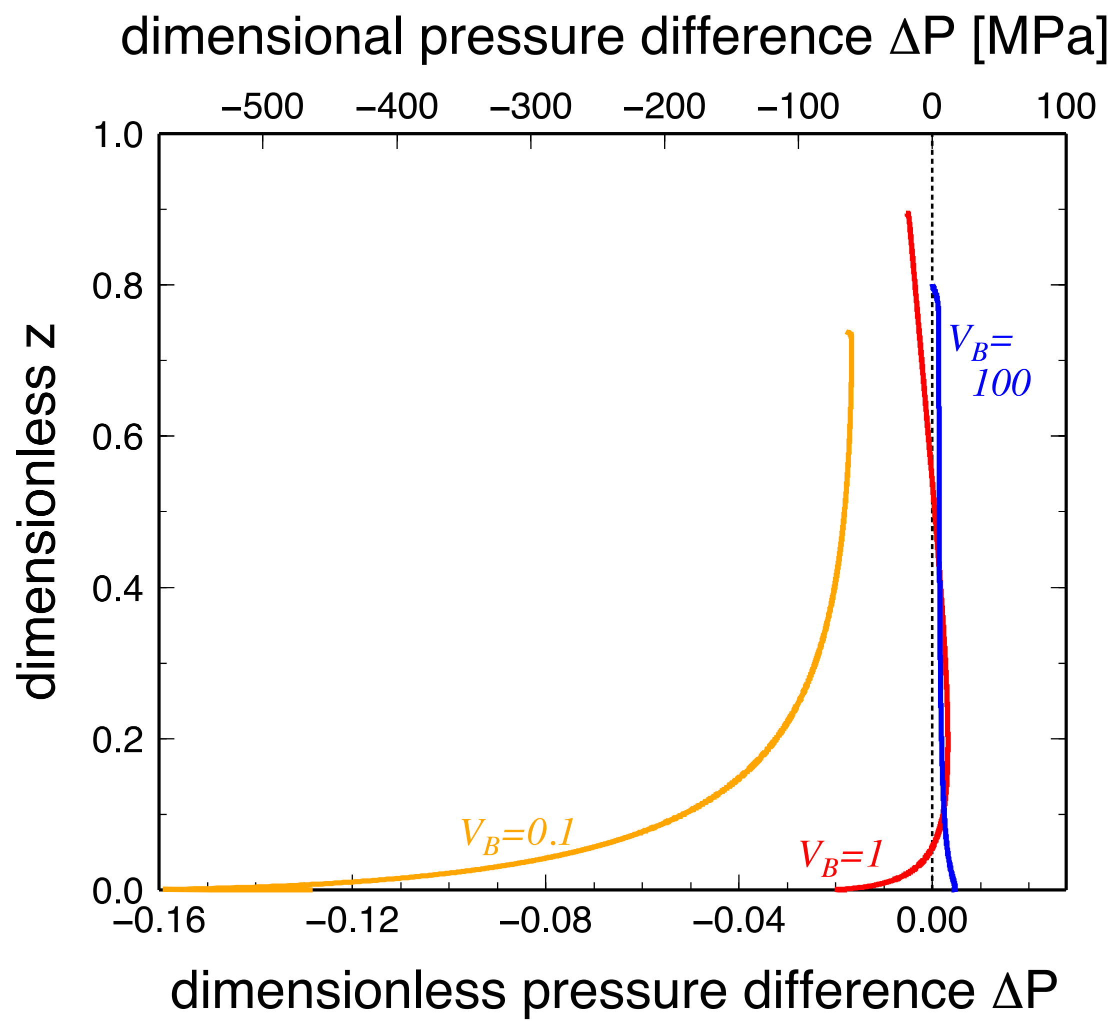

plotted for δ=0.26

Differentiation – dimensionless equations

divergence-free average velocity

$$\boldsymbol{\nabla} \cdot \overline{\mathbf{v}} = 0 \quad \text{where} \quad \overline{\mathbf{v}} = \phi \mathbf{v}_f + (1-\phi)\mathbf{v}_m = \mathbf{v}_m - \phi \boldsymbol{\Delta} \mathbf{v}$$

mometum equation for the mixture

$$-\boldsymbol{\nabla}\Pi + \boldsymbol{\nabla} \cdot (\mu^* \underline{\boldsymbol{\tau}}_m) + \phi \hat{\mathbf{g}} = 0$$

segregation velocity

$$\phi \boldsymbol{\Delta} \mathbf{v} = \delta^2 \phi^2 \left[\boldsymbol{\nabla} \left(\Pi + \frac{1-\phi}{\phi} \boldsymbol{\nabla} \cdot (\phi \boldsymbol{\Delta} \mathbf{v}) \right) - \hat{\mathbf{g}} \right]$$

$$\boldsymbol{\nabla}\widetilde{\Pi} = \boldsymbol{\nabla}\overline{P} - \rho_m \mathbf{g}$$

$$\mu^* = 1 - \phi$$

$$\delta^2 = \frac{\mu_m}{c a^2}$$

evolution of porosity

$$\frac{\partial \phi}{\partial t} + \overline{\mathbf{v}} \cdot \boldsymbol{\nabla} \phi = \boldsymbol{\nabla} \cdot [(1-\phi)\phi \boldsymbol{\Delta} \mathbf{v}]$$

energy equation

$$\frac{\partial T}{\partial t} + \overline{\mathbf{v}} \cdot \boldsymbol{\nabla} T = \frac{\nabla^2 T}{Ra} + \frac{\boldsymbol{\Delta} \mathbf{v}^2}{\delta^2} + \frac{1-\phi}{\phi} (\boldsymbol{\nabla} \cdot \mathbf{v}_m)^2 + \mu^* \underline{\boldsymbol{\tau}}_m : \boldsymbol{\nabla} \mathbf{v}_m$$

$$Ra = \frac{\overline{\rho C} |\Delta \rho| g a^3}{k_T \mu_m}$$

1-D spherically symmetric case

all the metal is liquid
only mechanical equations solved

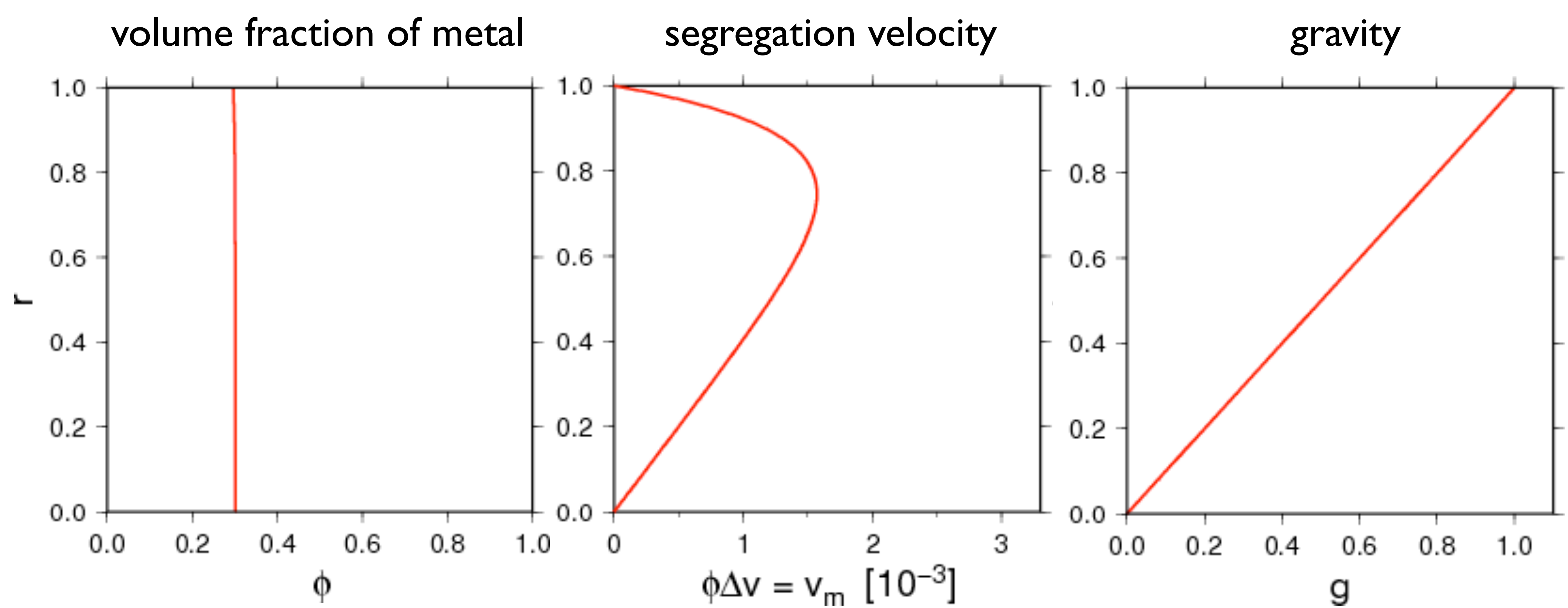

(δ=0.2)

1-D spherically symmetric case

all the metal is liquid
only mechanical equations solved

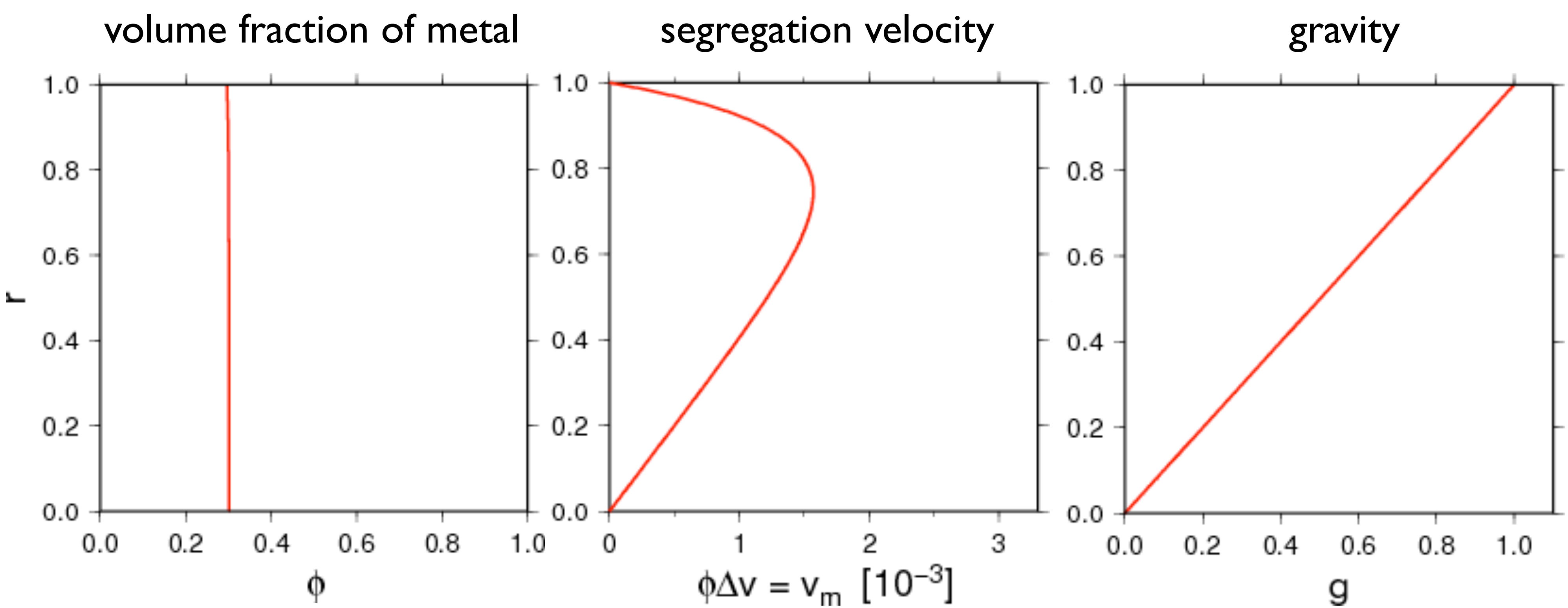

dimensionless compaction length δ=0.2

1-D spherically symmetric case

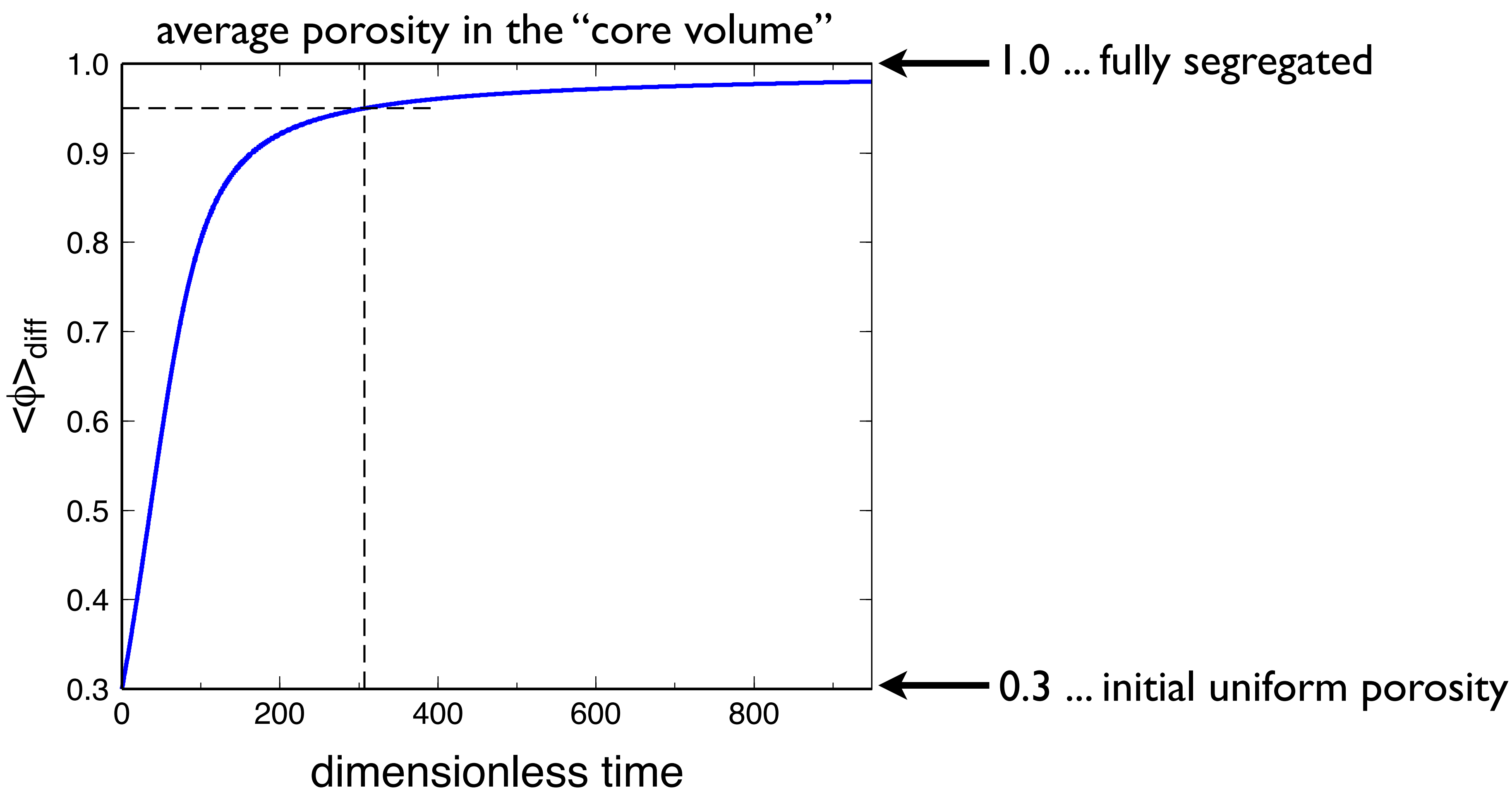

unit dimensionless time τ ~ 300 yr ...

core segregation time ~ 100 kyr

$$\tau = \frac{\mu_m}{|\Delta\rho| g_0 R}$$

Differentiation – numerical resolution

- guess $\nabla \cdot v_m$
- solve Navier-Stokes, direct, ∇^4-type
- solve phase separation, ADI relax., ∇^2-type
- solve compressible velocity, direct, ∇^2-type
- new $\nabla \cdot v_m$
- update porosity and temperature, superbee TVD

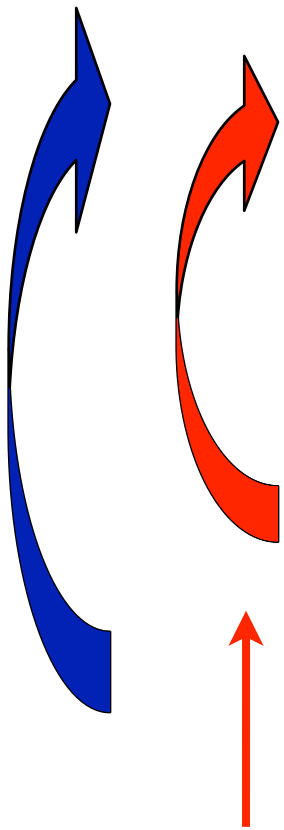

if $\mu^* = 1 - \phi$

Parameters – model of differentiation

silicate density	ρ_m		3200	$\mathrm{kg\,m^{-3}}$
iron density	ρ_f		7000	$\mathrm{kg\,m^{-3}}$
heat capacity	C		1000	$\mathrm{J\,K^{-1}\,kg^{-1}}$
thermal conductivity	k_T		3	$\mathrm{W\,m^{-1}\,K^{-1}}$
thermal expansion coeff.	α		$2\,10^{-5}$	$\mathrm{K^{-1}}$
reference temperature	T_0		1100	K
iron melting temperature	T_{melt}		1300	K
silicate viscosity	μ_m		10^{19}	Pa s
solid iron viscosity	μ_m		10^{19}	Pa s
liquid iron viscosity	μ_f		1	Pa s
permeability coeff. (eq. 1.12)	k_0		10^{-8}	$\mathrm{m^2}$
permeability exp. (eq. 1.12)	n		2	
initial porosity	ϕ_0		0.3	
density difference	$\lvert\Delta\rho^0\rvert$	$\lvert\rho_m^0 - \rho_f^0\rvert$	3800	$\mathrm{kg\,m^{-3}}$
initial average density	$\overline{\rho}_0$	$\rho_f\phi_0 + \rho_m(1-\phi_0)$	4340	$\mathrm{kg\,m^{-3}}$
ref. gravity (sph. body)	g_0	$4\pi G\overline{\rho}_0 a/3$	1.9	$\mathrm{m\,s^{-2}}$
length scale	a		1600	km
velocity scale	V	$\lvert\Delta\rho^0\rvert g_0 a^2/\mu_m$	60	$\mathrm{km\,yr^{-1}}$
time scale	τ	$\mu_m/(\lvert\Delta\rho^0\rvert g_0 a)$	270	yr
pressure scale	Π_0	$\lvert\Delta\rho^0\rvert g_0 a$	12	GPa
temperature scale	θ	$\lvert\Delta\rho^0\rvert g_0 a/(\overline{\rho C})$	2700	K
dimensional compaction length		$\sqrt{\mu_m/c}$	320	km
Rayleigh number	Ra	$\overline{\rho C}\lvert\Delta\rho^0\rvert g_0 a^3/(k_T\mu_m)$	$4\,10^9$	
compaction length	δ	$\sqrt{\mu_m/(ca^2)}$	0.2	
buoyancy number (mixture)	B	$\overline{\rho\alpha} g_0 a/(\overline{\rho C})$	0.06	
buoyancy number (liquid phase)	B_f	$\rho_f^0\alpha_f g_0 a/(\overline{\rho C})$		
sign of density difference	s	$\Delta\rho^0/\lvert\Delta\rho^0\rvert$	-1	

Impact heating

$$\Delta T_1 = \frac{4\pi f_1}{3 f_2} \frac{\bar{\rho}^2 G R^2}{\overline{\rho C}}.$$

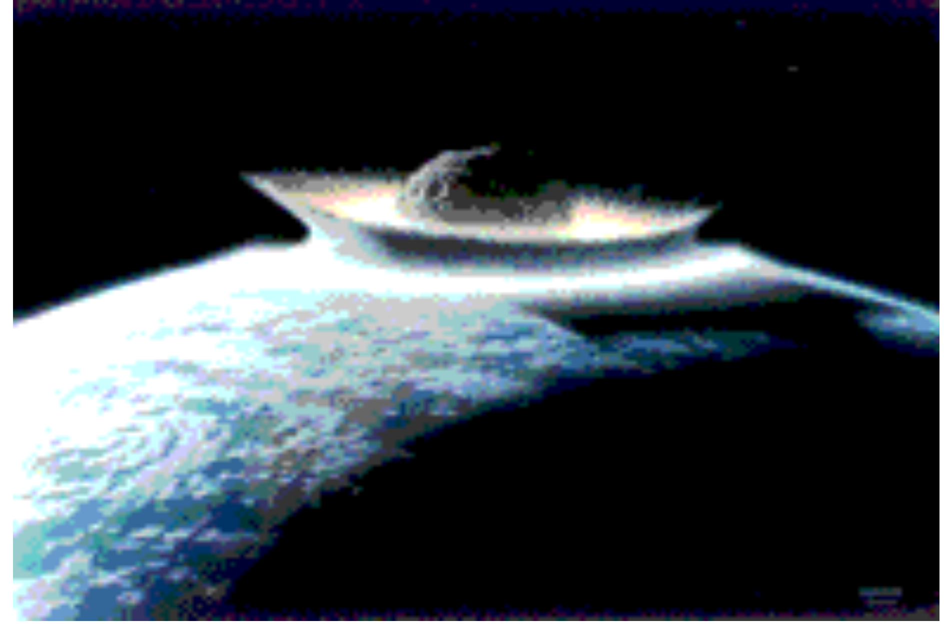

Differentiation heating

$$\Delta T_2 = \frac{4G\pi R^2}{5\overline{\rho C}} \left(\bar{\rho}^2 - \rho_f^2 \phi^{5/3} - \rho_m^2 (1 - \phi^{5/3}) - \frac{5}{2}(\rho_f - \rho_m)\rho_m \phi (1 - \phi^{2/3}) \right).$$

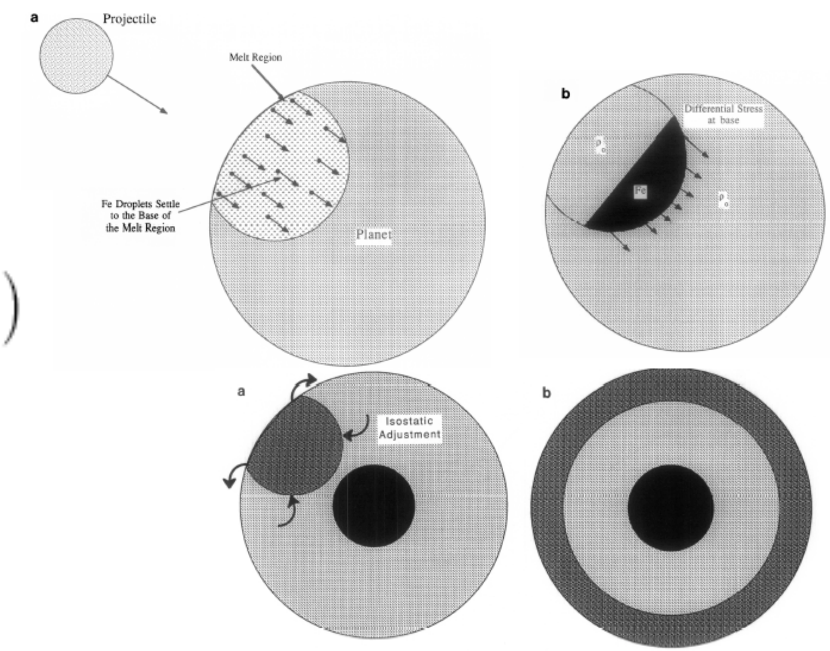

The two times are $\propto R^2$, and amount to 150 K for R=1500 km

Numerical test

$$\frac{d}{dt}\int_{\tilde{V}}(T-\phi z)\,dV = Q$$

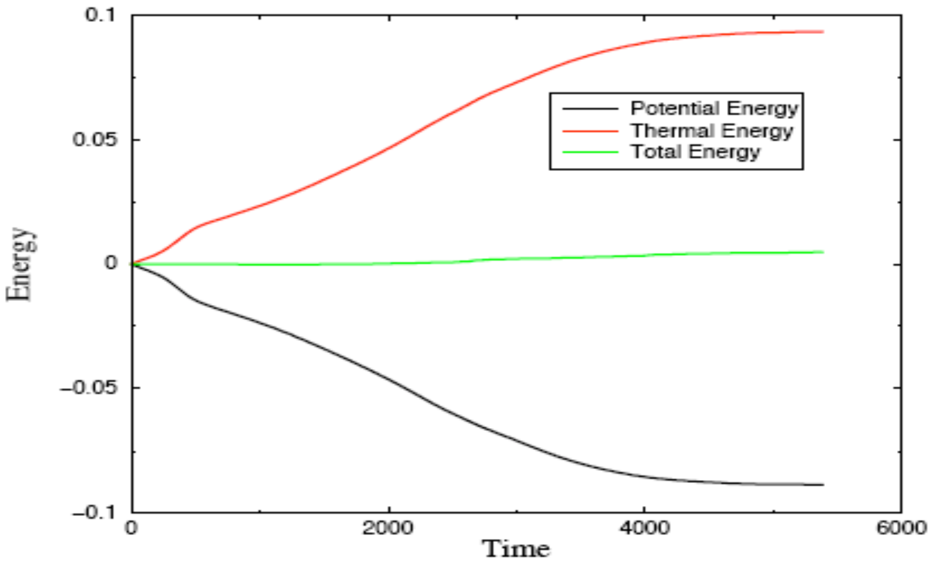

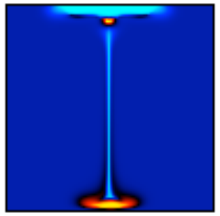

129x129

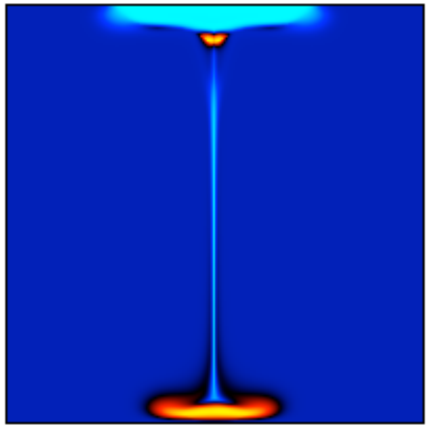

257x257

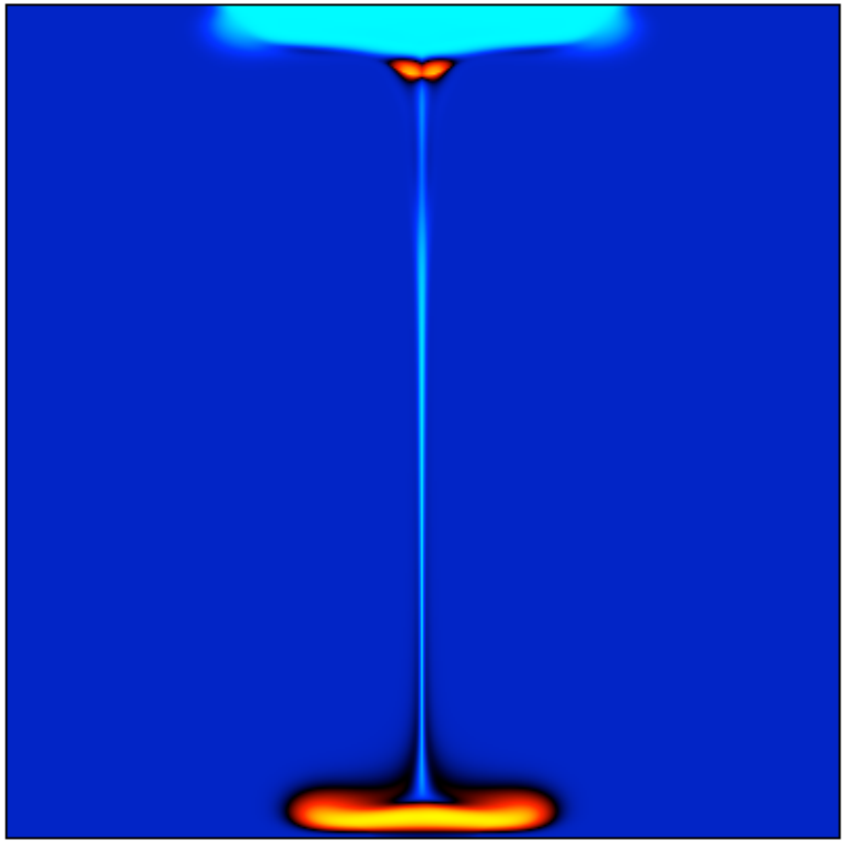

513x513

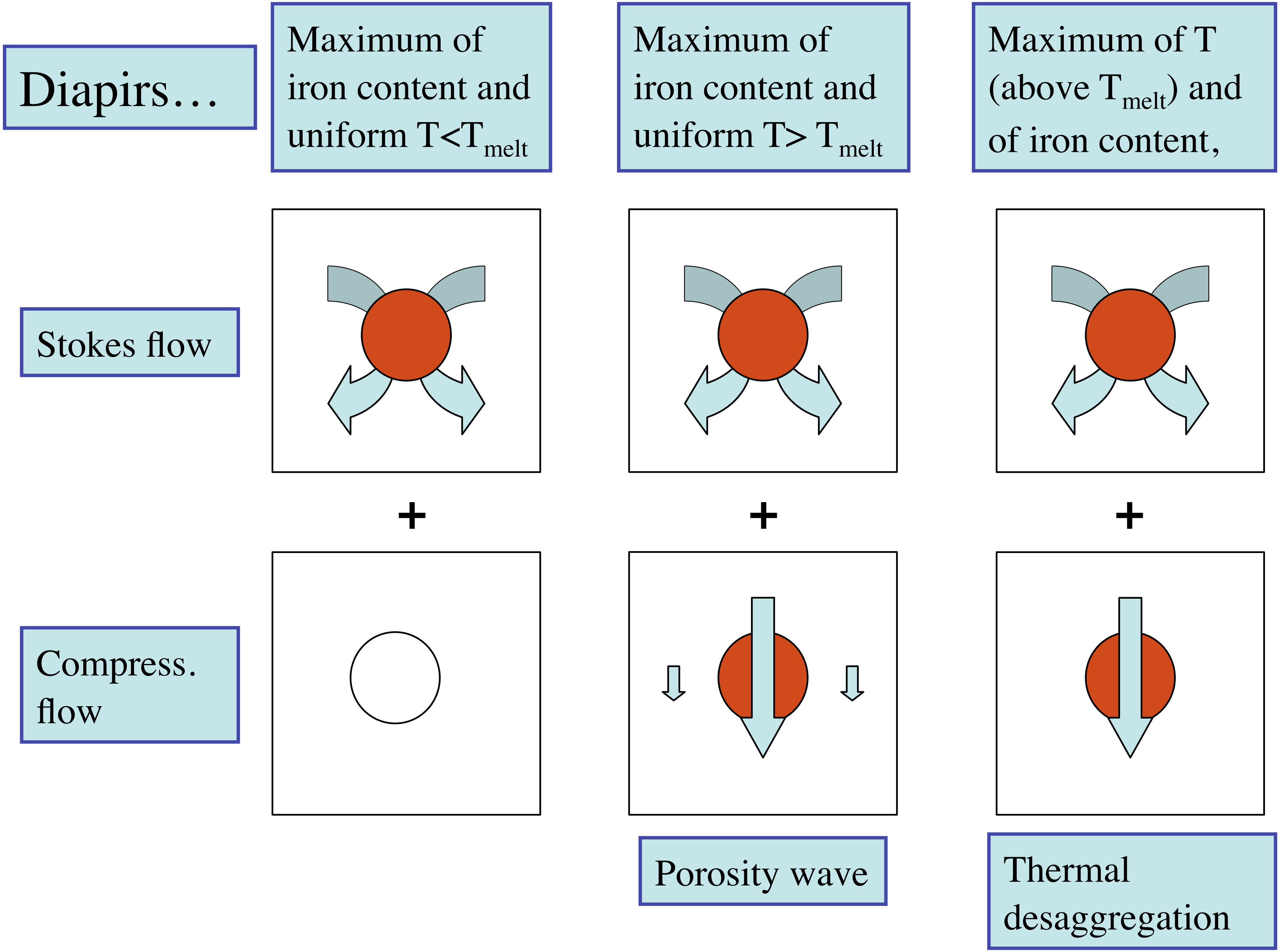

Diapirs…
Maximum of iron content and uniform $T<T_{melt}$
Maximum of iron content and uniform $T> T_{melt}$
Maximum of T (above T_{melt}) and of iron content,
Stokes flow
+
+
+
Compress. flow
Porosity wave
Thermal desaggregation

When does the instability develop?

the planet has to be hot enough
the impact has to be large enough

vary initial planetary temperature

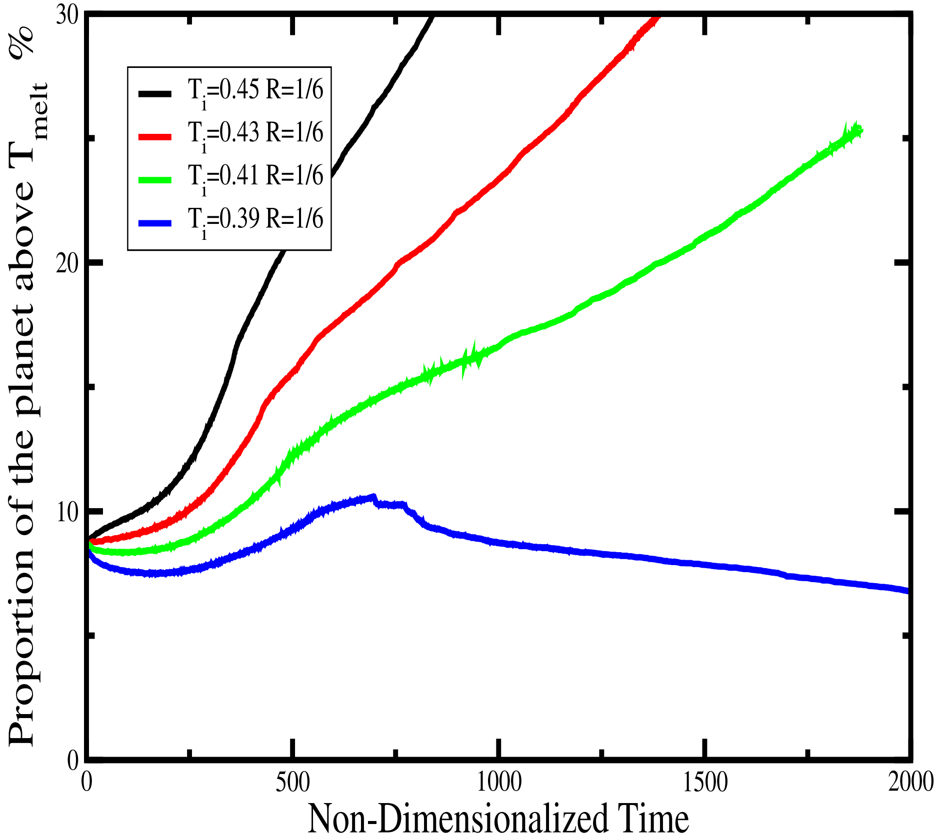

vary radius of the impacted zone

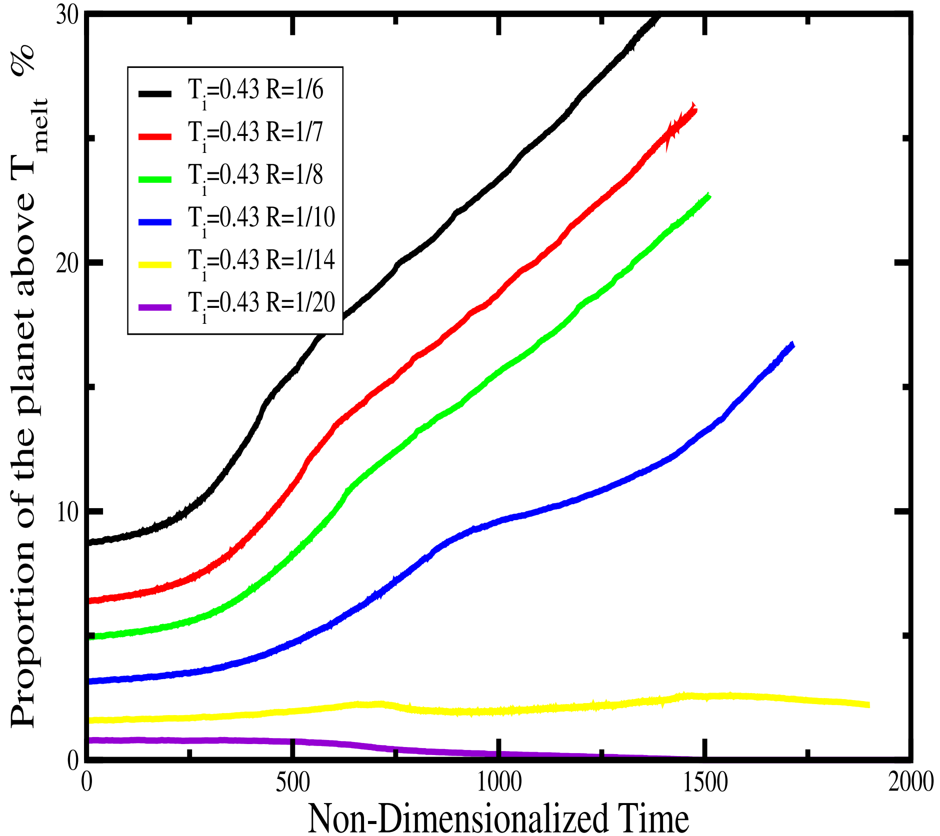

T_{melt} = 0.48 (1300 K), ΔT = 0.1 (270 K)

Forcing
Magma–solid density difference

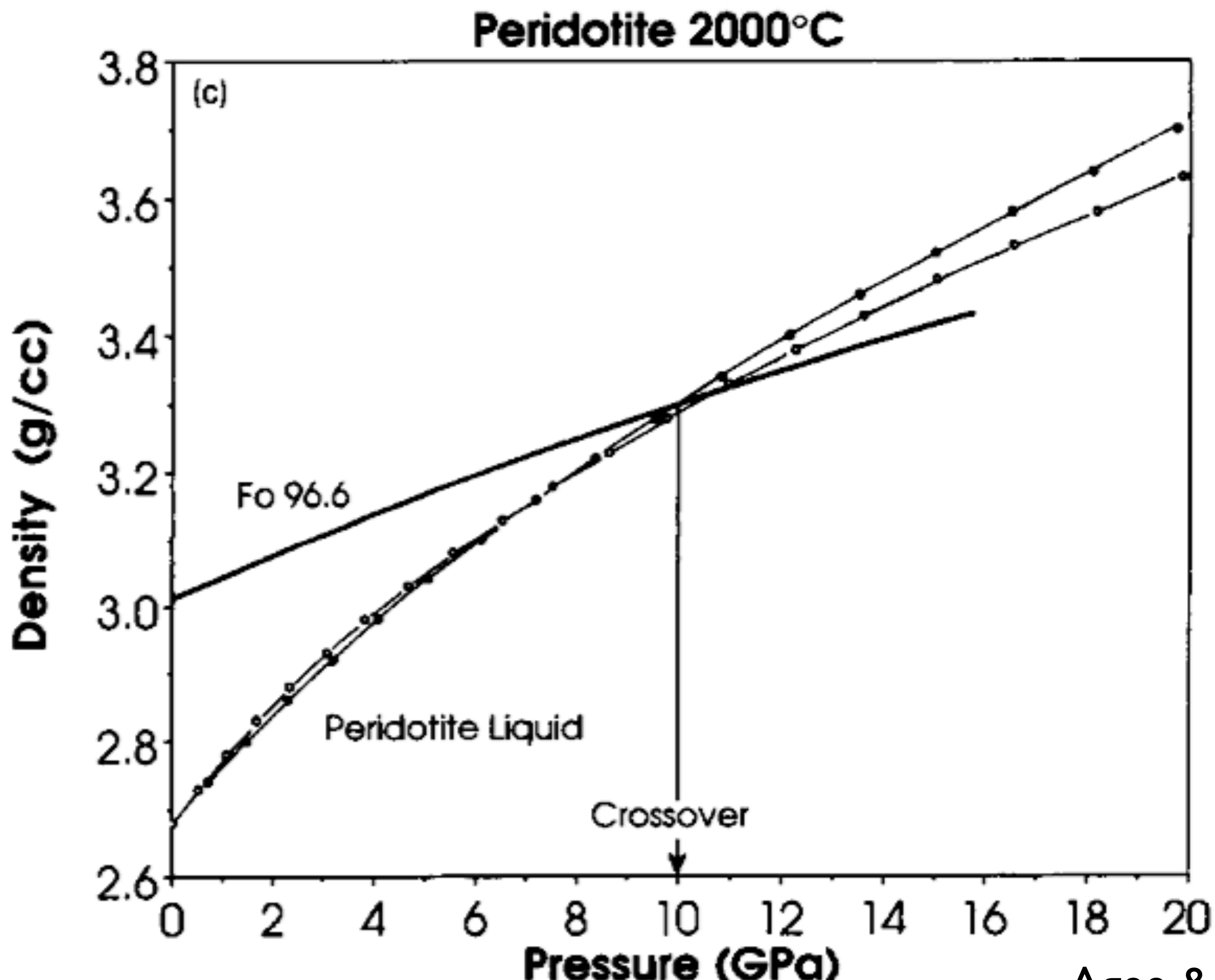

Agee & Walker (1993)

Magma migration in the Earth interior

- McKenzie's model has been widely used, standard for melt migration

spreading centers

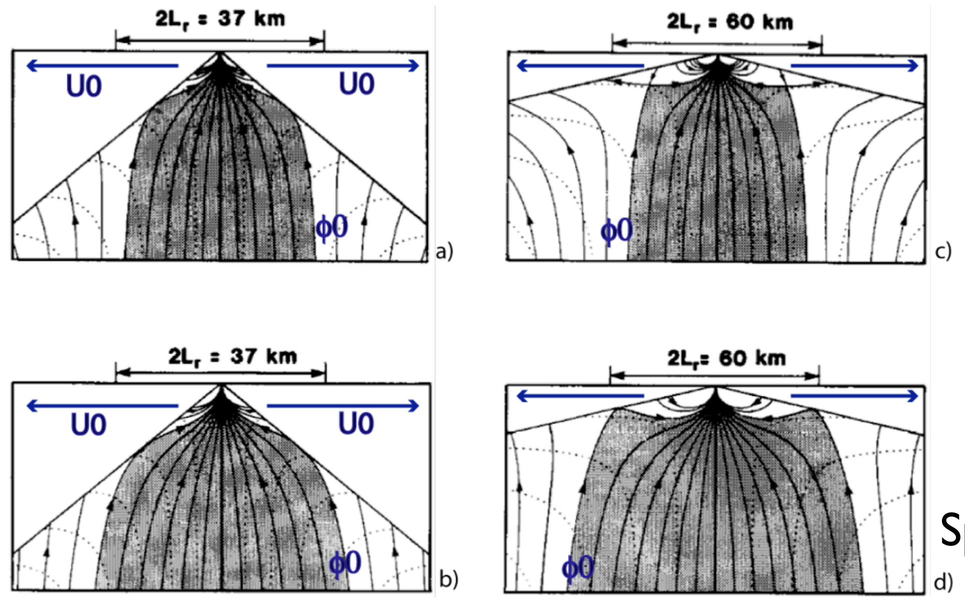

Spiegelman & McKenzie (1987)

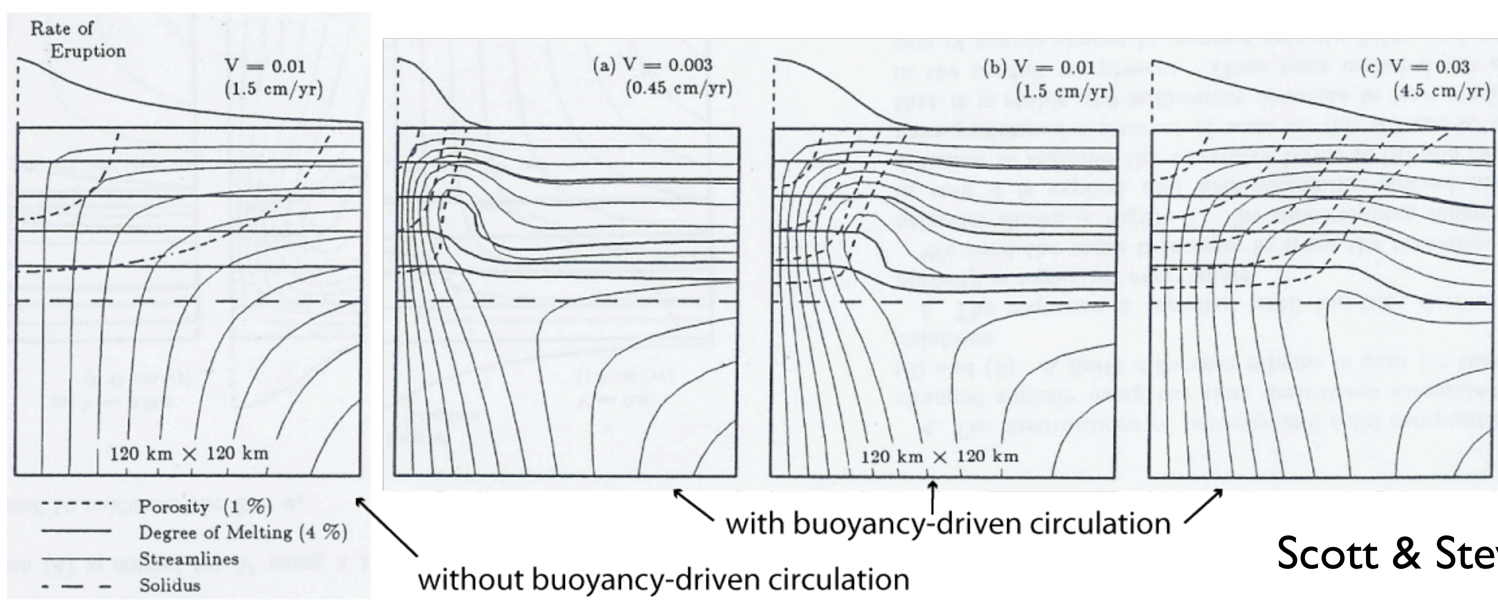

Scott & Stevenson (1989)

Momentum equations

• inertial terms neglected

force balance for the mixture

$$-\nabla \overline{P} + \nabla \cdot \underline{\overline{\tau}} + \overline{\rho}\mathbf{g} + \nabla(\sigma\alpha) = 0$$

average force exerted on the mixture by the interfaces

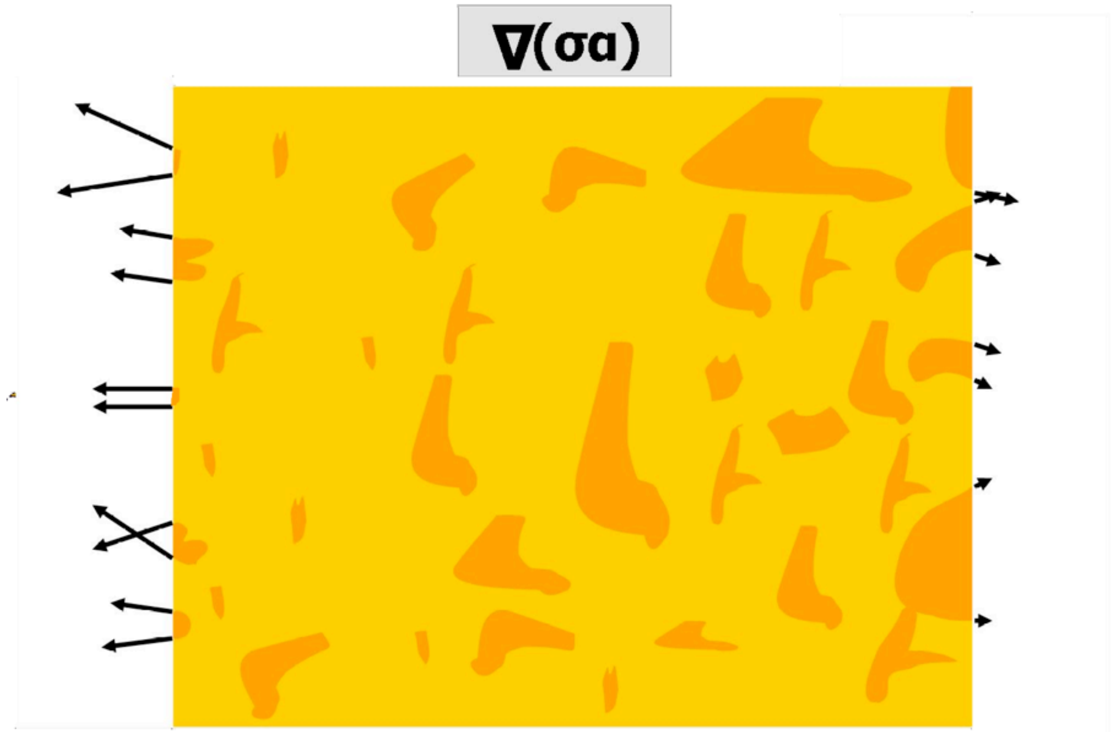

Porosity

- (single-phase) continuum mechanics:
  continuum assumption, “averaging” over microscopic (atomic scale) distribution of mass ⇒ density continuous in space

- two-phase continuum mechanics:
  additional “mesoscopic” scale of pores/grains of each phase
  ⇒ porosity continuous in space

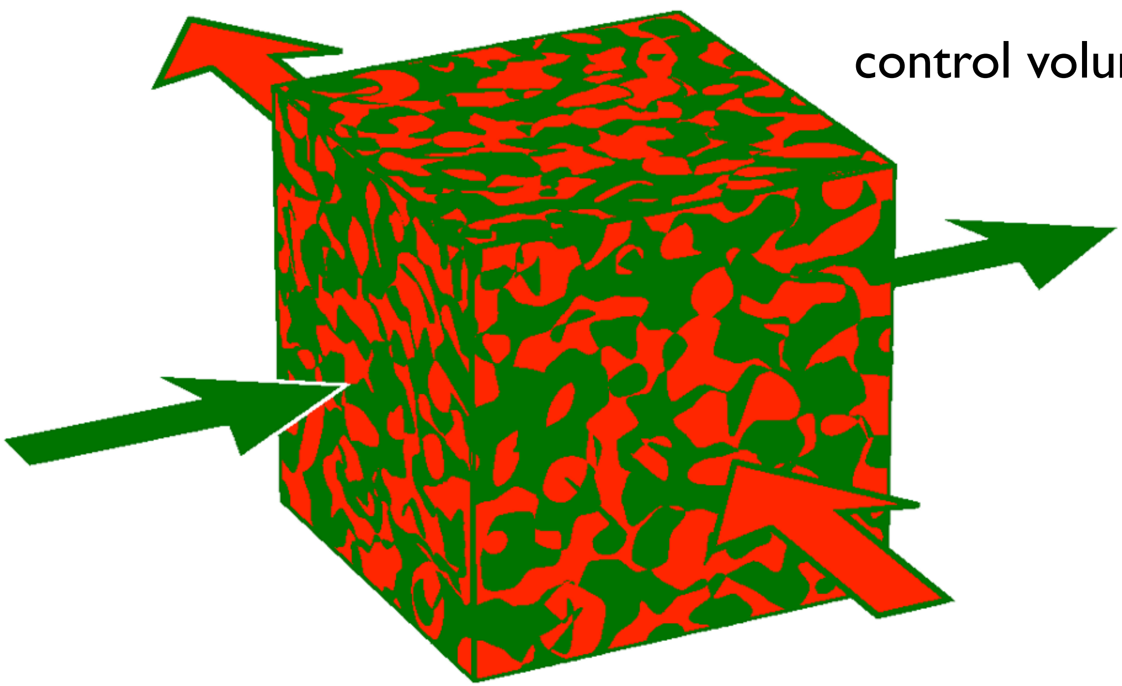

control volume

porosity

$$\phi(\mathbf{r},t) = \frac{1}{V_\mathrm{r}} \int_{V_\mathrm{r}} \theta(\mathbf{r}',t)\mathrm{d}\mathbf{r}'$$

Percolation, porous flow
Darcy's Law

Henry Darcy, mid 1800s
Construction of the Dijon municipal water system

immobile, non-deforming matrix
fluid flow due to hydrostatic pressure

$$\frac{\text{flux of water}}{\text{area}} = K \times \frac{\text{height of water column}}{\text{distance traveled through sand}}$$

$$\mathbf{v}_D = -\frac{k}{\mu}\nabla P$$

Darcy's Law

matrix permeability (k)

Darcy velocity ($\mathbf{v}_D$)

fluid viscosity (μ)

need interconnected fluid network

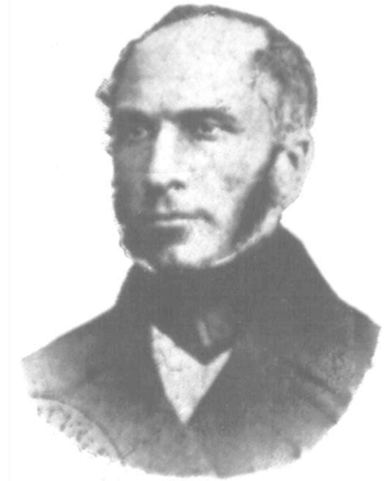

Figure 1. Portrait of Henry Darcy by F. Perrodin, from the Collection of the Bibliothèque Municipale de Dijon.